JOB MARKET PAPER
Adaptive Algorithms and Collusion via Coupling[*]

Martino Banchio Giacomo Mantegazza[†]

Stanford Graduate School of Business

October 19, 2022

PRELIMINARY: Click here for the latest version

Abstract

We develop a theoretical model to study strategic interactions between adaptive learning algorithms. Applying continuous-time techniques, we uncover the mechanism responsible for collusion between Artificial Intelligence algorithms documented by recent experimental evidence. We show that inadvertent coupling between the algorithms' estimates leads to periodic coordination on actions that are more profitable than static Nash equilibria. A new parameter, the relative learning rate, generates this coupling.: collusion disappears when the learning rates are uniform. We apply our results to the design of *learning-robust truthful mechanisms*, which guarantee implementation robust to the presence of learning agents. Robustness relies on ex-post feedback provision, which sidesteps inadvertent coordination between learning agents by allowing counterfactual evaluations. We identify optimal learning-robust mechanisms, which communicate personalized menu prices, in a class of canonical design problems.

Keywords: Artificial Intelligence, Learning, Mechanism Design, Continuous Time
JEL Classification Codes: C62, D47, D83, L51

[*]We are thankful to Anirudha Balasubramanian, Kostas Bimpikis, Emilio Calvano, Peter DeMarzo, Andreas Haupt, David Kreps, Irene Lo, Alexander MacKay, Paul Milgrom, Ilan Morgenstern, Evan Munro, Michael Ostrovsky, Andrzej Skrzypacz, Stefan Wager, Larry Wein, Gabriel Weintraub, Kuang Xu and seminar participants at Stanford University, Harvard University, IIOC, and SITE Conference.

[†]Email: mbanchio@stanford.edu, giacomom@stanford.edu

1 Introduction

Scholars and practitioners alike have expressed concerns that automated pricing and bidding software facilitates collusion. Simulations show how such software can learn sophisticated stick-and-carrot strategies (Calvano et al. (2020)), and empirical evidence shows prices in retail markets suffer a sharp increase after the introduction of automated pricing (Assad et al. (2021)). Motivated by these concerns, various national agencies have begun studying these phenomena to regulate and tune online and offline markets (OECD (2017), Competition Bureau (2018)).

Regulators and market design practitioners generally rely on theoretical models to guide policy interventions. The consensus in collusion analysis is that improvements in monitoring technology, as well as in response times simplify collusive agreements, making the case for a high risk of algorithmic collusion. Yet, as noted by Kühn and Tadelis (2018), tacit collusion requires independent algorithms to solve a coordination problem. Spontaneous coordination does arise between algorithms enjoying substantial success in single-agent environments, but their interactions in strategic environments remain puzzling. Although the theory surrounding markets with algorithmic agents has seen tremendous growth in the last few years, it still suffers from several challenges.[1] In this paper, we argue that the existing theory developed for rational agents is not suitable for learning algorithms, which adapt and evolve over time. Regulators and mechanism designers face a new challenge: the takeaways from industrial organization and implementation theory are not robust to the presence of learning agents.

We contribute to the analysis of algorithmic collusion by developing a theoretical framework for the analysis of strategic interactions between algorithms. Using fluid limit techniques, we approximate the evolution of algorithms driven by discontinuous laws of motion. The resulting dynamical system reveals the source of collusive behavior. A form of "coupling" between independent algorithms undermines the incentives for competition. The coupling originates from a characteristic of the algorithm, its relative learning rates. Uneven learning rates are responsible for introducing bias in the agent's estimates, sustaining long periods of correlated play.

We show that algorithms with uniform learning rates do not engage in collusive practices. We apply this result to construct a theory of learning-robust mechanism design. A designer may equalize learning rates by ensuring that agents can infer counterfactuals. In imperfect information settings the designer must reduce information asymmetry by providing feedback. Optimal learning-robust mechanisms select an outcome and release just

[1]See Tuyls and Weiss (2012) for a review of outstanding issues in the field of multi-agent learning.

enough information for every participant to compute counterfactuals. We design pVCG, a learning-robust mechanism that implements the social optimum. pVCG provides ex-post personalized menu pricing as feedback and thus guarantees simple counterfactual evaluations with minimal information disclosure.

We focus on learning algorithms, which adapt rapidly to market conditions and have found ubiquitous market applications. In both retail pricing and online auctions, pricing and bidding algorithms need to quickly react to changes in demand and competition, often without direct human supervision. Because of their adaptive nature, learning algorithms are an ideal tool for decision-making in these contexts. We characterize a class of such adaptive algorithms, which we call *reinforcers*: they learn by inflating estimates of successful actions and deflating unsuccessful ones. Various popular automated decision software fall into this category, and their adaptive structure allows us to construct a continuous-time approximation. The piecewise-smooth system approximating the evolution of the algorithms is tractable enough for us to characterize its equilibria and regions of attraction.

We provide an example in which two AI algorithms (Q-learning) learn to cooperate in a Prisoner's Dilemma. The simulation shows that, even in a dominant-strategy-solvable game, algorithms may fail to reach equilibrium. We reconstruct analytically the results and prove that algorithms inadvertently coordinate on dominated actions. Intuitively, during a period of joint cooperation, each agent's estimates are correct if the opponent is also cooperating. Experimenting with defection appears profitable in the short run. However, the coupled agents soon begin to jointly defect, and the estimated value of defection falls. Instead, the estimate of cooperation remains high, luring the algorithms away from defection. We dub this phenomenon the coordination bias, highlighting how nearly simultaneous deviations sustain dominated outcomes.

Inadvertent algorithmic coupling proves more general. The coordination bias arises when an agent learns about some actions faster than others. A single parameter for each action, the relative learning rate, determines the presence of coordination bias and inadvertent collusion. Actions with high relative speed adjust quickly to new information. Conversely, actions with slow relative speed take much longer to be re-assessed. Different persistence of estimates impairs the ability of a learning agent to adapt its behavior in response to strategic incentives.

The coordination bias disappears when agents observe the unrealized payoffs of neglected actions. Counterfactuals allow agents to update each action in lockstep, and persistence is uniform across all actions. While computing counterfactuals could itself be challenging, various environments make it impossible. For example, an agent's private information may determine her opponent's price. In imperfect information settings, the evaluation of counterfactuals relies on information that may not be public. However, markets can develop disclosure policies that guarantee access to all unrealized payoffs. Market designers have control over the release of the private information gathered at any stage of the mechanism.

We formalize the notion of learning-robust truthful implementation: we require both adaptive and rational agents to report their private information truthfully. We show that implementation is achieved by jointly designing the allocation mechanism and a feedback structure. A generic strategy-proof implementation might fail without ex-post feedback to help algorithms learn — learning-robust mechanisms provide such feedback. We can augment any mechanism with a feedback structure to make it learning-robust. These mechanisms are ordered according to the degree of information they reveal to their participants. We look for the optimal learning-robust mechanism, which discloses the least private information to all participants. We characterize the maximally-private mechanism for efficient implementation with quasi-linear utilities. Optimal feedback takes the form of personalized menu pricing. Each choice from the menu corresponds to a price for a given outcome, simplifying counterfactual evaluations.

Finally, we show that experimental results found in the literature can be derived analytically within our framework. We apply our model to a recent paper by Asker et al. (2022). In a simulated Bertrand oligopoly, the authors find that different learning rules can lead to either competition or collusion. By exploiting our results, we can show that their algorithms reach competition only when they have access to counterfactual profits. We then repeat the same analysis in the context of auctions studied in Banchio and Skrzypacz (2022).

The paper is structured as follows: in the next Section we review the related literature; in Section 2 we introduce the theoretical framework and derive the approximation results. In Section 3 we present a complete analysis of a Prisoner's Dilemma and we build intuitions that we generalize in Section 4 to various settings. In Section 5 we employ these results to establish a theory of learning-robust mechanisms, and we finally apply our results in Sections 6.2 and 6.3 to the Bertrand pricing of Asker et al. (2022) and the auctions of Banchio and Skrzypacz (2022).

1.1 Literature Review

Q-learning and Artificial Intelligence have recently sparked interest in Economics, often through experimental work (see e.g. Klein (2021), Hansen et al. (2021), Banchio and

Skrzypacz (2022)) or empirical work (see e.g. Musolff (2021), Assad et al. (2021)). The work of Calvano et al. (2020) draws attention to strategies as a proxy for collusion: they argue that simply looking at outcomes of learning might be insufficient, as collusion might arise as a "mistake" by poorly designed algorithms. Our work allows to delve deeper into the dynamics of learning, and through comparative statics and convergence analysis determine whether collusion is systemic. Particularly relevant is the work by Asker et al. (2022), which analyzes the impact of algorithm design on collusion in a Bertrand pricing game, and by Banchio and Skrzypacz (2022), who find that additional feedback in first-price auctions restores competition. We contribute to these questions with analytical tools that allow us to generalize their intuition and prove that counterfactual information guarantees competition in the games they consider. Some papers analyze models of collusion between algorithms, for example Brown and MacKay (2021), Leisten (2022), and Lamba and Zhuk (2022). In these papers, algorithms choose prices based on the opponent's last quoted price: the strategies are Markov, which rules out many plausible learning strategies, including most AI algorithms. We focus on *learning* algorithms, which adapt their decisions along the whole history. Contributions from the bandit literature include Aouad and Van den Boer (2021), who prove tacit collusion schemes arise with classical multi-armed bandits algorithms, and Hansen et al. (2021), which finds supra-competitive prices are sustained by coordinated experiments when bidders use the Upper Confidence Bound algorithm. We prove our results for general classes of algorithms, allowing for heterogeneity in parameters as well as algorithms themselves.

Some work has examined more generally Reinforcement Learning in games, for example Erev and Roth (1998) or Mertikopoulos and Sandholm (2016), but with some notable differences. Firstly, many have analyzed systems experimentally (Erev et al. (1999), Lerer and Peysakhovich (2017)). Our approach is complementary: with the aid of our framework, one can tell apart experimental findings from agent design considerations. On the other hand, there is some theoretical work on convergence of learning procedures. For example, learning through reinforcement has been associated with evolutionary game theory by Börgers and Sarin (1997). Others have formally analyzed some of the simpler models, as Hopkins and Posch (2005). These results have then been extended to more complex systems, but with a focus on the connection with replicator dynamics as their core. Our approach is particularly relevant because instead it examines the workhorse model in applied work, ε-greedy Q-learning. We obtain a tool valuable for regulation and design, but we trade it off against the complete understanding possible in a simpler system. Conveniently, the approach described in Section 2 includes some earlier results under a general algorithmic structure.

Some earlier work analyzes continuous-time approximation of AI algorithms, mostly in the single-agent setting. Related to ours is the work of Tuyls et al. (2005): the authors examine a continuous-time approximation of multi-agent Q-learning with Boltzmann exploration, and show a link with the Replicator Dynamics from the Evolutionary Game Theory (EGT) literature. Building on their work, Leonardos and Piliouras (2022) characterize the tradeoff between exploration and exploitation in the same setting. Our approximations and results hold in more general settings: we analyze a general class of adaptive algorithms, and our results leverage their discontinuities. Both Gomes and Kowalczyk (2009) and Wunder et al. (2010) propose a continuous-time approximation of Q-learning in a multi-agent setting with ε-greedy algorithms. Their approximations are mutually inconsistent and require additional conditions on the parameter. Most importantly, those approximations remain model-dependent. Our method applies to general adaptive algorithms. The result is a recipe to analyze equilibria through the lens of dynamical systems, abstaining from heuristic modeling choices. The work of Benaim (1996) often serves as a foundation for stochastic approximations in learning. With respect to our approach, those tools have a harder time handling general learning procedures, including AI techniques that fall under the umbrella of Temporal Difference Learning. Additionally, we adopt the formalism of differential inclusions to analyze points of non-differentiability, generally new to the theory of stochastic approximations.[2]

Fluid models and other forms of approximation have enjoyed great popularity in the fields of applied probability and operations research. Starting from the seminal contributions of Iglehart (1965), Kurtz (1970), Halfin and Whitt (1981) and Harrison and Reiman (1981), approximations enabled formal analysis of systems otherwise deemed intractable: see, e.g., Wein (1992) for a classic application to inventory management. More recently, Mitzenmacher (2001) applied fluid models to the analysis of parallel computing systems, while Wager and Xu (2021) employ diffusion approximations to study sequential experiments.

We contribute to the theory of implementation in the presence of boundedly-rational agents. Abreu and Matsushima (1992) provides implementability in dominance-solvable games, but the iterative deletion of dominated strategies requires mixing, which our setting does not allow. A few papers consider implementation in supermodular games, which could be adopted in our model (see Chen (2002) and Mathevet (2010)). Sandholm (2005) develops implementation in potential games, as this class guarantees valuable evolutionary properties. We suspect similar results would hold under our framework. All of

[2]One exception is the paper by Wunder et al. (2010), which however abandons this route in favor of simulations.

these works provide robustness to certain types of bounded rationality and learning procedures. As we show, the robustness guaranteed by the game form may be insufficient — even the strongest strategy-proof incentives fail to guarantee implementation. We instead add a new lever, feedback provision, to the toolbox of the designer.

2 Model

We begin by describing a general class of algorithms we call *reinforcers*: they learn by reinforcing successful actions and penalizing unsuccessful ones. Because their dynamics tend to be complex, we approximate these algorithms in continuous time with ordinary differential equations (ODEs).

2.1 Games with Adaptive Agents

Consider a finite normal-form game $G = (N, (A_i)_{i \in N}, (r^i)_{i \in N})$ with N players. We are interested in what happens when agents play repeatedly in this game by choosing actions using a learning algorithm. For simplicity, let us look at one agent, Alice, choosing her actions from the finite set A_i with cardinality d_i. Instead of selecting an action herself, Alice delegates the decision-making to an algorithm that tries to learn how to maximize her utility. The function $r_i(a_i, a_{-i})$ describes her utility, which depends on her opponents' actions and her own.

For example, Alice might take actions as recommended by a well-known AI algorithm, ε-greedy Q-learning.

Example 1. *A ε-greedy Q-learning algorithm consists of a vector $Q(k)$ for every period k and a decision rule π_ε.*

- *Each entry $Q_a(k)$ is an estimate of the long-run value of action $a \in A$. The update for entry $Q_a(k+1)$ in period $k+1$ is given by*

$$Q_a(k+1) = \begin{cases} Q_a(k) + \alpha\left[r(k) + \gamma \max_{a'} Q_{a'}(k) - Q_a(k)\right] & \text{if } a = a(k) \\ Q_a(k) & \text{else.} \end{cases} \tag{1}$$

  where $r(k)$ is the payoff and $a(k)$ is the action the algorithm took in period k. $\gamma \in [0,1)$ is a discount factor, and $\alpha \in (0,1)$ is called learning rate.

- *Given the vector $Q(k)$, the algorithm takes actions according to a ε-greedy policy. The* *decision rule $\pi_\varepsilon : \mathbb{R}^{|A|} \to \Delta(A)$ selects the following probability distribution over actions:*

$$\pi_\varepsilon(Q(k)) = \begin{cases} \dfrac{1}{|\text{argmax}_{a\in A_i} \theta^a|} & \forall a \in \text{argmax}_{a\in A_i} Q_a(k) \quad \textit{with probability } 1-\varepsilon \\ \frac{1}{d_i} & \forall a \in A_i \quad \textit{with probability } \varepsilon \end{cases}$$

The Q vector is a more general version of the Erev and Roth (1998) and Börgers and Sarin (1997) reinforcement learning models. We analyze in this work a different, more straightforward decision rule. The ε-greedy policy offers an intuitive recipe for resolving the tradeoff between exploration and exploitation. With probability $1-\varepsilon$ the algorithm is *greedy*: it selects the action corresponding to the largest entry of the Q vector. The algorithm exploits what he considers to be the best action at the time. With probability ε it explores the entire action space by taking an action at random.

Intuitively, the Q-vector estimates the long-run value of actions by iterating over a Bellman equation. In period k, the value of an action at a certain state is a convex combination of its previous estimate (with weight $1-\alpha$) and a new Bellman estimate (with weight α). The weight α serves as a learning rate, and we can interpret it as a measure of persistence: higher αs make the algorithm faster in forgetting the past.

Most Q-learning-based methods belong to a larger class of adaptive algorithms that we name reinforcers.

Definition 1. A *reinforcer* for agent i is a pair (θ^i, π^i) consisting of

- A d_i-dimensional stochastic process θ^i that evolves according to

$$\theta^i(k+1) = \theta^i(k) + \alpha^i T^i(a_i(k), r^i(k), \theta^i(k)),$$

  where $a_i(k) \in A_i$ is the action taken by agent i in period k, $\theta^i \in K \subset \mathbb{R}^{d_i}$, and $\alpha^i \in \mathbb{R}_+^{d_i}$ are learning rates for all actions $a_i \in A_i$.

- A *policy* π^i, that is a map $\pi^i : K \to \Delta(A_i)$, which selects a distribution of actions for each value of the process $\theta^i \in K$.

A reinforcer carries a statistic for each available action and selects an action in period k according to its policy. Both agent i's and her opponents' policies introduce randomness in the process θ^i. The update function T^i depends Alice's realized actions directly and on her opponents' actions through her utility. To completely define a reinforcer, we need to specify also an initial value of $\theta^i(0)$, which we call the *initialization* of θ^i. We maintain the following assumption on the update function T^i:

Assumption A1. The functions $T^i(a_i, r, \theta)$ and $\pi^i(\theta)$ are Lipschitz-continuous almost-everywhere in θ.

Let us return to Example 1. The policy π_ε is constant on the subspace of $\mathbb{R}^{d_i}$ where $\mathrm{argmax}_a \theta^i_a$ is fixed and unique. The argmax changes only along the lines of the form $\left\{\theta^i | \theta^i_a = \theta^i_{a'} = \max \theta^i\right\}$, which have zero Lebesgue measure. The discontinuities of the update function of Q lie on the same lines, and thus the update is also a.e. Lipschitz. The ε-greedy Q-learning satisfies Assumption A1.

When multiple agents employ reinforcers, we represent the system as a single vector of dimension $d_1 \cdot \dots \cdot d_N$ by stacking the individual algorithms, denoted by $\theta(k) = (\theta^1(k), \dots, \theta^N(k))$. Similarly, T and π indicate the collection of update functions and policies when missing a superscript.

2.2 Approximation in Continuous Time

We are interested in describing the dynamics of learning for a given reinforcer. A common feature of reinforcers is that while relatively simple to analyze in a stationary environment, they often become unpredictable when learning to play against each other. For example, Q-learning is known to converge in stationary, single-decision-maker environments. In strategic settings, if all opponent's actions were constant, ε-greedy Q-learning would learn how to best respond. However, when opponents are themselves non-stationary, its properties are all but well understood. Analyzing the learning path of any number of Q-learning agents requires describing discrete, possibly stochastic updates and how those interact over time.

This section proposes a continuous-time approach to deal with the two former difficulties. We adopt the formalism of fluid approximations first introduced by Kurtz (1970). The idea behind fluid approximations is to analyze the limit of the systems as the jumps get small and their frequency increases. The limiting fluid ODE system provides tractability and (often) closed-form solutions.

The first step in formalizing the approximation consists of *Poissonizing* the stochastic vector θ associated with a reinforcer. That is, we consider a Poisson clock with rate $\lambda_1 = 1$. On average, the clock ticks once in a unit of time. At every tick of the Poisson clock, the now continuous process $\theta_1(t)$ gets updated according to the vector function T. The Poissonized process $\theta_1(t)$ is a compound Poisson process. We introduced a new layer of randomness, but the path traced by $\theta^1(t)$ remains identical to the path of the discrete $\theta(t)$.

We can now generate a sequence of processes $(\theta_n)_{n\in\mathbb{N}}$ by increasing the rate of the Poisson clock to $\lambda_n = n$. The goal is to regularize the learning dynamics; therefore, we need to compensate for frequent updates by reducing the size of the jumps. We do this by dividing each jump by $\frac{1}{n}$: in the parlance of Definition 1, at a given arrival time τ of the Poisson process,

$$\theta(\tau) = \theta(\tau^-) + \frac{\alpha}{n} T(a(\tau^-), r_{\tau^-}, \theta(\tau^-)).$$

Each process θ_n has the same infinitesimal generator: the sequence $(\theta^n)_{n\in\mathbb{N}}$ preserves the instantaneous rate of change throughout. We can prove the following result:

Theorem 1. *Let $H \subset K$ be such that T and π are Lipschitz over H, and let $y_0 \in H$ be the initialization point of θ. Then, the sequence of continuous-time stochastic processes $(\theta_n)_{n\in\mathbb{N}}$ converges in probability to the solution of the following Cauchy problem:*

$$\begin{cases} \frac{d\Theta^i(t)}{dt} = \alpha \mathbb{E}_{\pi^i,\pi^{-i}}\left[T^i(\pi^i, r(\pi^i,\pi^{-i}), \Theta^i(t))\right] \\ \Theta^i(0) = y_0^i \end{cases}$$

for all i. That is, $\lim_{n\to\infty} P\left\{\sup_{t\le T}\left\|\theta^n(t) - \Theta(t)\right\| > \eta\right\} = 0$ for all $T \ge 0$ and $\eta > 0$ such that $\{\Theta(t)\}_{t\le T} \subset H$.

We provide a formal proof of this result in Appendix A. The process $\Theta(t)$ for $t \ge 0$ is the fluid approximation to θ: it is a deterministic dynamical system whose time-derivative is the expected update that the discrete process θ_k would incur over one unit of time. Theorem 1 guarantees that the sequence of processes $(\theta_n)_{n\in\mathbb{N}}$ we constructed draws closer and closer (in probability) to the continuous process. The theorem relies on a law-of-large-numbers argument: if the updates occur with high frequency and each update's contribution is relatively small, the process behaves similarly to its expectation. We leverage the fundamental theorem of fluid approximations by Kurtz (1970), a stochastic-processes version of the law of large numbers, to conclude convergence in probability.

2.3 Continuous-Time Dynamical Systems

Instead of analyzing the discrete reinforcers, we focus on their continuous-time fluid limits. Their dynamical system structure provides us with a wide range of tools to characterize their path over time.

Definition 2. Given a dynamical system $\frac{d\theta}{dt}$, the *flow* of θ starting in x is the map

$$\begin{array}{rccc} \theta(-,x)\colon & [0,+\infty) & \to & K \\ & t & \mapsto & \theta(t,x) \end{array}$$

that satisfies Equation (2) with initial condition $\theta(0,x) = x$. A *trajectory* of the dynamical system is the graph of the flow, $\Big\{(t,\theta(t,x))\colon\ t \in [0,+\infty)\Big\}$. The set $\Gamma_x = \Big\{\theta(t,x)\colon\ t \in [0,+\infty)\Big\}$ is the *orbit* of θ starting from x. If a sequence $(t_n)_{n\in\mathbb{N}}$ is such that

$$\begin{cases} \lim\limits_{n\to\infty} t_n = +\infty \\ \lim\limits_{n\to\infty} \theta(t_n,x) = y \end{cases}$$

we say that y belongs to the *forward limit set* for the orbit Γ_x. A *steady state* of the dynamical system is a fixed point of its law of motion, i.e. $\frac{d\theta}{dt}(t) = 0$.

The actions taken by a reinforcer depend directly on its estimates. Thus, analyzing the underlying dynamical system is a good proxy for the path of play. Studying the forward limit set of a reinforcer allows us to focus on estimated values instead of realized actions. A policy such as ε-greedy trembles organically: even if the reinforcer settles its estimates and identifies the action with the largest expected reward, it will keep playing sub-optimal actions (albeit with a small probability). The reinforcer can nonetheless become stationary if its estimates reach a steady state. We adopt this view for simplicity and clarity of exposition.

Definition 3. We say a reinforcer (θ^i,π^i) initialized at x *converges* if $\theta^i(t)$'s flow started at x converges on a steady-state $\overline{\theta}^i$. We say the agent *converges on action* a_{ss} if the steady-state $\overline{\theta}^i$ is such that $a_{\text{ss}} \in \text{argmax}_{a\in A_i} \overline{\theta}^i_a$. If the argmax is not unique, we say $\overline{\theta}^i$ is a *pseudo-steady-state*.

The requirement of existence of a steady state can, at times, be stringent, which is why we allow agents to learn an action a_l if the estimate of that action is always the largest in the limit.

Definition 4. We say the agent *learns action* a_l if there exists a $T > 0$ such that $a_l \in \text{argmax}_{a\in A} \theta^a(t)$ for all $t \geq T$. Equivalently, for all $\overline{\theta}$ in the forward limit set of a given orbit, $\overline{\theta}^{a_l} = \max_{a\in A} \overline{\theta}^a(t)$.

It is a simple exercise to show that if the forward limit set of θ is a singleton, an agent who learns action a_l also converges on action a_l. Importantly, an agent can learn action a_l

even if she doesn't play said action in each period. The definition of reinforcers is overly permissive, allowing for many procedures which do not behave well in their limit. For this reason, in the rest of the paper we focus on what we call *separable* reinforcers.

Definition 5. A reinforcer (θ^i, π^i) is said to be *separable* if the fluid approximation of θ^i is of the form

$$\frac{d\theta_a^i(t)}{dt} = \alpha_a^i\Big(\theta^i(t)\Big)\Big[U\Big(\theta_a^i(t), \mathbb{E}_{\pi_{-i}}[r^i(a, \pi_{-i})]\Big) + V\Big(\theta^i(t)\Big)\Big]. \tag{2}$$

where $\alpha_a^i(\theta^i) \in [0,1]$, α, U, and V are a.e. Lipschitz in all components, U is Lipschitz everywhere and increasing in $\mathbb{E}[r(a,\pi_{-i})]$ and decreasing in θ_a^i, and $\frac{\partial V}{\partial \theta^{a_i}} < -\frac{\partial U}{\partial \theta^{a_i}}$ almost everywhere.

Two parts make up a separable reinforcer: a component that is equal for all actions, $V(\theta^i)$, and a component that is action specific but Lipshitz over the entire domain K, $U(\theta_a^i, \mathbb{E}[r^i])$. The function U, uniform across all actions, operates on a given action's estimates. The first of the monotonicity assumptions amounts to requesting that a reinforcer's updates increase with good news. The second states that a reinforcer likes surprises: the update shrinks if the agent already holds an action in high regard.

Notice that we allow for heterogeneity in the learning rates α_a^i across actions. The heterogeneity accounts for differences in learning rates originating from the policy. The ε-greedy Q-learning described in Example 1 exemplifies this assumption.For Q-learning,

$$U(Q_a^i(t), \mathbb{E}[r^i]) = \mathbb{E}[r^i(a_i, \pi_{-i})] - Q_a^i(t)$$

and $V(Q^i)$ is simply $\gamma \max_a Q_a^i(t)$. Thus, U is linear in its arguments and Lipschitz everywhere, increasing in rewards and decreasing in $Q_a^i(t)$. The common component V is constant over its Lipschitz domains and since $\gamma < 1$ its derivative is dominated by U's. The learning rate $\alpha_a^i(\theta^i(t))$ in the case of ε-greedy Q-learning is simply $\alpha_a^i \cdot (\pi_\varepsilon(\theta^i(t)))_a$: the Q-learning rate α^i multiplied by the probability of selecting action a given $\theta^i(t)$.

The restriction to separable reinforcers does not rule out standard algorithms. Separability only requires that an algorithm "treats each action the same": the only term that can differ across actions is the learning rate α. All entries of the vector θ^i adopt the same action-specific component, and any interaction term appears uniformly in all actions' updates.

3 An Illustrative Example

We now analyze the behavior of separable reinforcers in a simple game with an equilibrium in dominant strategies. We find in simulations that reinforcers fail to learn the unique Nash equilibrium. We then apply continuous-time techniques to characterize the learning outcomes and identify the critical mechanism that prevents convergence on dominant strategies.

Consider the following family of contribution games, with payoffs given by Figure 1. Alice and Bob have two American dollars each, and they simultaneously decide whether or not to contribute to a shared pool that grows its value by a factor of $1 < g < 2$. The riches in the pool are then shared equally between Alice and Bob, but each agent gets to keep what they didn't contribute on top of that. This game is a canonical model of the free-rider problem. The parameter g models the attractiveness of joint cooperation: the larger g, the more attractive cooperation becomes. However, for all $g \in (1, 2)$, the dominant strategy, and the only Nash equilibrium, is to play “defect" and keep one's change.

$$\begin{array}{cc|c|c|}
 & & \multicolumn{2}{c}{\text{Bob}} \\
 & & C & D \\
\hline
\text{Alice} & C & 2g, 2g & g, 2+g \\
\hline
 & D & 2+g, g & 2, 2 \\
\hline
\end{array}$$

Figure 1: Payoffs of the stage game, $1 < g < 2$.

Simulations. We simulate the learning dynamics of Alice and Bob when they adopt ε-greedy Q-learning in the above free-rider problem. At each iteration k Alice and Bob play the action with the highest estimated value, i.e., $\operatorname{argmax}_{a \in \{C,D\}} Q_a(k)$, with probability $1-\varepsilon$, and with probability ε they choose an action uniformly at random.

Figure 2a shows the results of these numerical experiments. The algorithmic agents play the dominant strategy equilibrium $\{D, D\}$ only for low values of the parameter g. Instead, when g is large, the agents cooperate, albeit imperfectly. Both cooperation and defection appear in unpredictable but recurrent cycles, as shown in Figure 2b: the value of collaboration is generally above that of defection, but it drops below $Q_D(k)$ at somewhat regular intervals so that agents switch to playing D. The value of defection then decreases almost immediately, and players revert to cooperation. This analysis highlights a few puzzles. First, the parameter g should have no effect on strategic decisions, and

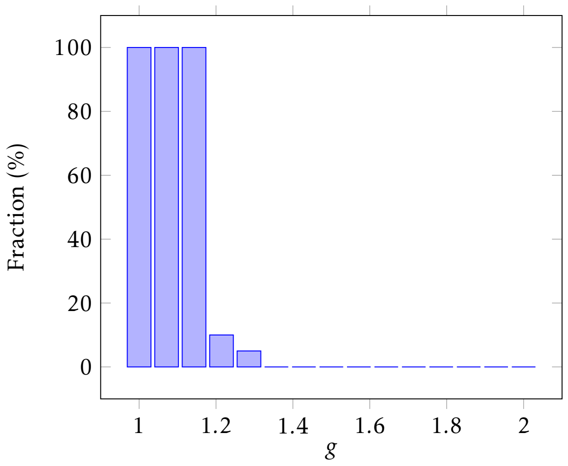

(a) Fraction of runs where the agents learn the Nash Equilibrium $\{D, D\}$.

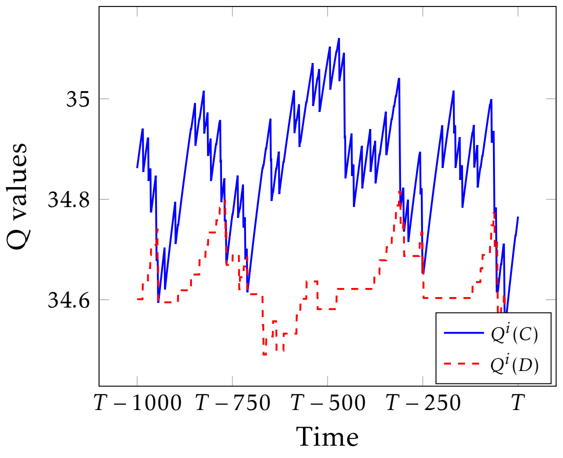

(b) Cycles in the discrete system, obtained with $g = 1.8$.

Figure 2: We initialized 100 independent runs of Q-learning with $T = 100,000$ time steps each. We say a profile (a_A, a_B) is learned if the corresponding Q-values are the largest in over 50% of the last 1000 iterations. We chose parameters $\varepsilon = 0.1$, $\alpha = 0.05$ and $\gamma = 0.9$. The initialization is optimistic, i.e. all Q-values are larger than the maximum value they could ever achieve. This leads to a phase of intense exploration at the outset.

instead it leads to stark differences in outcomes. Second, collusion seems to consist of cycles, but since agents cannot condition on the past action of the opponent, it is hard to impute these to “retaliatory" strategies. The continuous-time approximation describes both patterns and clarifies their origin.

3.1 Theoretical results

We begin the theoretical analysis by explicitly writing down the continuous-time approximation of ε-greedy Q-learning. When Alice and Bob adopt this algorithm, they learn only about the actions they take, which depend on the values of $Q(k)$. In the parlance of Definition 1, both Alice and Bob have a function T^i with a discontinuity along the surface $Q^i_D(k) = Q^i_C(k)$. To sidestep this discontinuity in the right-hand side of the discrete-time system, we first apply Theorem 1 to $Q(k)$ over the largest open sets such that $T = (T^A, T^B)$ is everywhere Lipschitz. We call these sets *maximal continuity domains*: in the case of ε-greedy Q-learning these are sets $\omega_{a,b}$ of vectors Q such that Alice's greedy action is a and Bob's greedy action is b.

Over $\omega_{C,C}$ the greedy action for both players is C, so that in every period Alice cooperates with probability[3] $1-\frac{\varepsilon}{2}$ and defects with probability $\frac{\varepsilon}{2}$. Hence, with probability $(1-\frac{\varepsilon}{2})^2$ she collects reward $2g$ — similarly for other profiles. Therefore, the fluid limit in $\omega_{C,C}$ solves

$$\begin{cases} \dfrac{d\mathbf{Q}_C^A(t)}{dt} = \alpha\left(1-\dfrac{\varepsilon}{2}\right)\left[\left(1-\dfrac{\varepsilon}{2}\right)2g+\dfrac{\varepsilon}{2}g+(\gamma-1)\mathbf{Q}_C^A(t)\right] \\ \dfrac{d\mathbf{Q}_D^A(t)}{dt} = \alpha\dfrac{\varepsilon}{2}\left[\left(1-\dfrac{\varepsilon}{2}\right)(2+g)+2\dfrac{\varepsilon}{2}+\gamma\mathbf{Q}_C^A(t)-\mathbf{Q}_D^i(t)\right] \\ \dfrac{d\mathbf{Q}_C^B(t)}{dt} = \alpha\left(1-\dfrac{\varepsilon}{2}\right)\left[\left(1-\dfrac{\varepsilon}{2}\right)2g+\dfrac{\varepsilon}{2}g+(\gamma-1)\mathbf{Q}_C^B(t)\right] \\ \dfrac{d\mathbf{Q}_D^B(t)}{dt} = \alpha\dfrac{\varepsilon}{2}\left[\left(1-\dfrac{\varepsilon}{2}\right)(2+g)+2\dfrac{\varepsilon}{2}+\gamma\mathbf{Q}_C^B(t)-\mathbf{Q}_D^i(t)\right] \end{cases} \tag{3}$$

Similar systems appear in all continuity domains, and can be written in matrix form as

$$\dot{\mathbf{Q}}(t) = \begin{cases} A_{C,C}\mathbf{Q}(t)+b_{C,C} \text{ for } \mathbf{Q}(t)\in\omega_{C,C} \\ A_{C,D}\mathbf{Q}(t)+b_{C,D} \text{ for } \mathbf{Q}(t)\in\omega_{C,D} \\ A_{D,C}\mathbf{Q}(t)+b_{D,C} \text{ for } \mathbf{Q}(t)\in\omega_{D,C} \\ A_{D,D}\mathbf{Q}(t)+b_{D,D} \text{ for } \mathbf{Q}(t)\in\omega_{D,D} \end{cases} \tag{4}$$

The behavior of this 4-dimensional piecewise-linear system with 4 right-hand sides turns out to be complex. In particular, the system exhibits chaotic behavior over various parametrizations and initial conditions (see Appendix B for more details on chaos theory and its analysis in the contribution game).

To make progress in the analysis of the chaotic system, we begin by restricting attention to a subspace of $\mathbb{R}^4$. In particular, we note that if the initial condition is symmetric, the system is bound to remain symmetric: the space $\{Q\in\mathbb{R}^4 | Q_a^A = Q_a^B \text{ for } a = C, D\} \cong \mathbb{R}^2$ is a subspace for the dynamical system in Equation (4). In what follows, we will then make the following assumption:

Assumption S. Let $\mathbf{Q}_a^A(0) = \mathbf{Q}_a^B(0)$ for $a = C, D$.

Under Assumption S, we can prove the following proposition, which characterizes the limiting behavior of the continuous-time approximation.

Proposition 1. *There always exists a steady-state $q_D^{eq}\in\omega_{D,D}$. Moreover, if $\varepsilon < 1-\sqrt{\frac{2-g}{g}}$ there*

[3]I.e., C is selected with probability $1-\varepsilon$ if the randomization device instructed the agent to be greedy and with probability $\frac{\varepsilon}{2}$ if the agent plays a random action.

exists a pseudo-steady-state $q_C^{eq} \in \overline{\omega}_{D,D} \cap \overline{\omega}_{C,C}$, given by

$$q_C^{eq}(C) = q_C^{eq}(D) = \frac{1 + g + \sqrt{(g-1)(g-1-\varepsilon g + \frac{\varepsilon^2 g}{2})}}{(1-\gamma)}.$$

In the symmetric subspace, the limiting behavior of the system can be twofold. When ε is larger than the critical level $\underline{\varepsilon}(g) = 1 - \sqrt{\frac{2-g}{g}}$, the algorithms converge on a steady state q_D^{eq} where both players find defection to be the preferred action. However, when ε is below the critical level, an additional steady state exists. Recall Definition 3: this pseudo-steady-state q_C^{eq} lies at the intersection of the sets where Alice and Bob prefer cooperation and defection. In this steady state, Alice and Bob play cooperation only a fraction τ of the time and defect for a fraction $1 - \tau$ of the time.

Corollary 1. *In the pseudo-steady-state q_C^{eq} agents spend τ_c fraction of their time cooperating, where*

$$\tau = \frac{\frac{\varepsilon^2 g}{2} + \varepsilon - 2 - q_C^{eq}(\gamma-1)(1-\varepsilon)}{2(\varepsilon-1)(1+g+(\gamma-1)q_C^{eq})} \in \left[\frac{1}{2}, 1\right].$$

The pseudo-steady-state q_C^{eq} corresponds to the imperfect cooperation we observed in the experiments. In particular, the analytic expression for the time spent cooperating approximates its discrete-time experimental counterpart closely, as shown in Figure 6b. Moreover, we observe that the general asymmetric 4-D system gravitates around a similar equilibrium, where $Q_C = Q_D$.

We will spend the following subsection constructing the necessary tools to formally prove Proposition 1 and its corollary.

3.2 Sketch of the proofs

Recall that under Assumption S the system can evolve according to one of the following two equations:

$$\dot{\mathbf{Q}}(t) = \begin{cases} A_{C,C}\mathbf{Q}(t) + b_{C,C} \text{ for } \mathbf{Q}(t) \in \omega_{C,C} \\ A_{D,D}\mathbf{Q}(t) + b_{D,D} \text{ for } \mathbf{Q}(t) \in \omega_{D,D} \end{cases}$$

We denote the two vector fields over each domain $\omega_{a,a}$ as F_a for $a \in \{C, D\}$. The flows within each $\omega_{a,a}$ characterize the evolution of the Q-functions. The system at large however is discontinuous: we would like to preserve continuity of any given flow along the boundary $\overline{\omega}_{C,C} \cap \overline{\omega}_{D,D}$. Proposition 2 below guarantees that we can suitably extend the flows on the boundary, similarly to continuous pasting techniques, such that the flow defined by the fluid limit is globally defined forward in time.

Proposition 2. *Let F_a be the field defined as above over $\omega_{a,a}$ for all $a \in \{C, D\}$. There exists a global solution in the sense of Filippov (1988) to the differential inclusion*

$$\begin{aligned} \frac{d\mathbf{Q}_t}{dt} &= F_a(\mathbf{Q}_t) && \text{over } \omega_{a,a} \text{ for } a = C, D \\ \frac{d\mathbf{Q}_t}{dt} &\in co\Big\{F_a(\mathbf{Q}_t)\Big|\ \forall a = C, D\Big\} && \text{when } \mathbf{Q}_t \in \overline{\omega}_{C,C} \cap \overline{\omega_D, D} \end{aligned}$$

where $co\{\cdot\}$ denotes the convex hull of a set, and $\overline{\omega}$ is the closure of ω.

Both vector fields F_C and F_D are well-defined also on the boundary between $\omega_{C,C}$ and $\omega_{D,D}$. This boundary is called a *switching surface*, because the laws of motion must switch from one field to the other. Adopting the Filippov convention, we can define a vector field on the switching surface such that all flows extend to a global solution.

Let us call $\hat{\mathbf{N}}$ the unit normal vector to the switching surface $\overline{\omega}_{C,C} \cap \overline{\omega_D, D}$. We divide the switching surface in three regions, according to the signs of the normal components of the two vector fields F_C and F_D. A *crossing region* occurs when both normal fields to the boundary $\hat{\mathbf{N}} \cdot F_a$ are of the same sign. Either F_C or F_D can be used to define the law of motion on the surface: any orbit leaves the switching boundary immediately. A *repulsive region* occurs where both normals $\hat{\mathbf{N}} \cdot F_a$ face away from the boundary, which will then never be reached. Unless initialized here, an orbit will never intersect the repulsive region, thus we do not need to define a field here. Finally, a *sliding region* occurs when both normal components $\hat{\mathbf{N}} \cdot F_a$ of the two vector fields point towards the boundary. Every flow hitting the switching surface in the sliding region must continue on the switching surface, *sliding along the boundary*. The sliding vector field is defined as a convex combination of the two vector fields F_C and F_D with parameter τ such that the normal component to the switching surface vanishes, i.e. $\tau(\hat{\mathbf{N}} \cdot F_C) + (1-\tau)(\hat{\mathbf{N}} \cdot F_D) = \vec{0}$. The vector field $\tau F_C + (1-\tau) F_D$ is the unique vector field in the convex hull of F_C and F_D whose flow is confined to the switching surface and which satisfies the differential inclusion requirements. Figure 3 plots the vector fields around the boundary and shows an example of sliding and crossing boundaries, together with a sample orbit. For more details on how the field is calculated we refer the reader to the proof of Proposition 1 in the Appendix.

Stability analysis Figure 4 shows the vector fields that characterize the continuous-time approximation: their orbits behave approximately as the original system. The figures highlight the presence of two stationary points when g is large. The pseudo-steady-

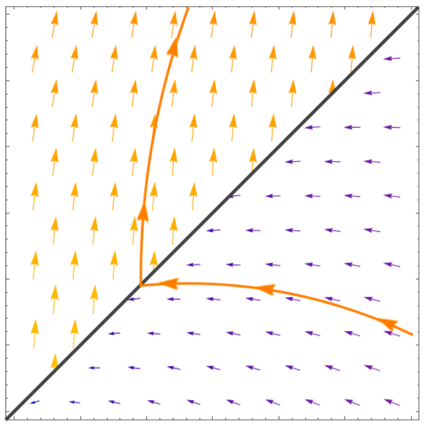
(a) Trajectory crossing the boundary.

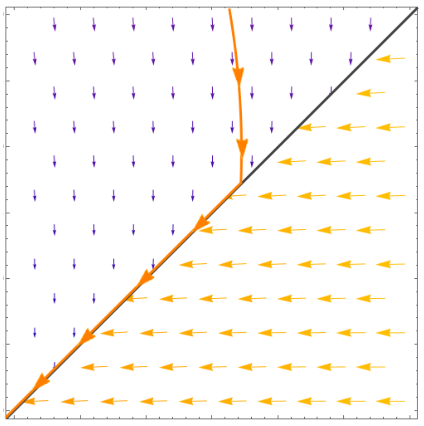
(b) Trajectory sliding along the boundary.

Figure 3: Depiction of two discontinuous flows around a switching surface, in the crossing and sliding case.

state on the boundary disappears for lower values of g. The analytical characterization of the two points mentioned in Proposition 1 follows the derivation in Appendix A.

We will refer to the point q_C^{eq} as the *cooperative equilibrium*. Its existence hinges on the relationship between the value of cooperation and the exploration rate. Figure 5 shows the minimum exploration $\underline{\varepsilon}$ that guarantees a cooperative equilibrium and how it varies with the value of cooperation. Intuitively, as g increases, the relative benefit of defecting decreases (and vanishes completely when $g = 2$), so more and more exploration is needed to realize that D is a dominant action. For example, if $g = 1.8$ the exploration rate required to guarantee convergence on $\{D, D\}$ is about 70%, which is considerably larger than the standard employed in practice.[4]

Sustaining cooperation Note that the system of ODE, when simulated with small but discrete time steps, closely mimics the path of play of the discrete Q-learning. We compare Figure 6a with Figure 2b, shedding some light on how cooperation could be sustained.

Suppose C is the preferred action of both players: Alice and Bob cooperate but with probability $\frac{\varepsilon}{2}$ one defects and realizes its benefit. Over time, Q_D^i is bound to rise above Q_C^i. Suppose this happens first to Alice. Once Alice defects, Bob will also defect almost immediately after, because cooperating when Alice defects makes Bob considerably worse off. Joint defection decreases the value of Q_D^i for Alice and Bob but changes the value of cooperation too slowly. Effectively, when the exploration rate is too small, the

[4]The literature on Q-learning in games usually employs $\varepsilon = 0.1$ or smaller, either fixed or decreasing over time. E.g., see Gomes and Kowalczyk (2009).

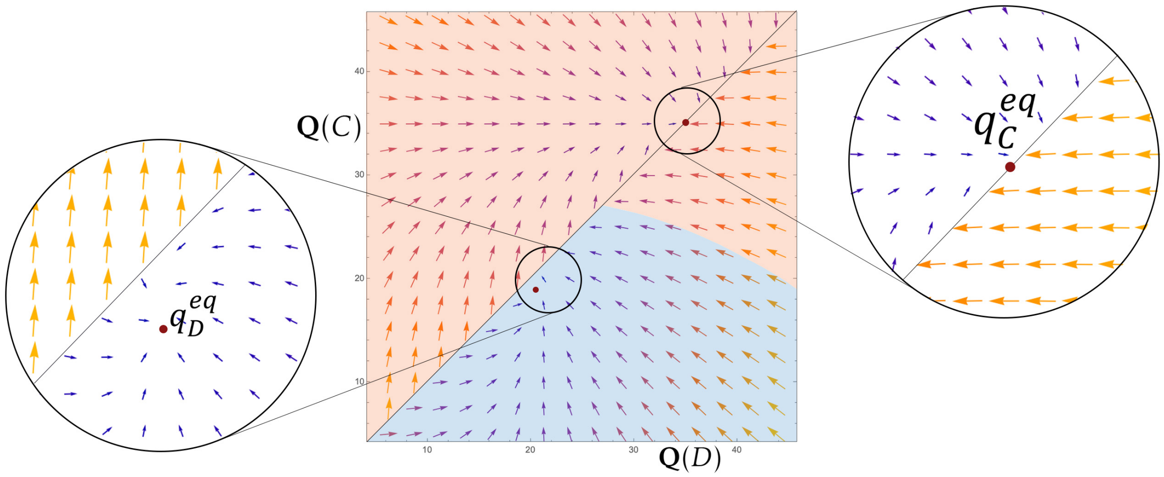

(a) Phase space with $g = 1.8$.

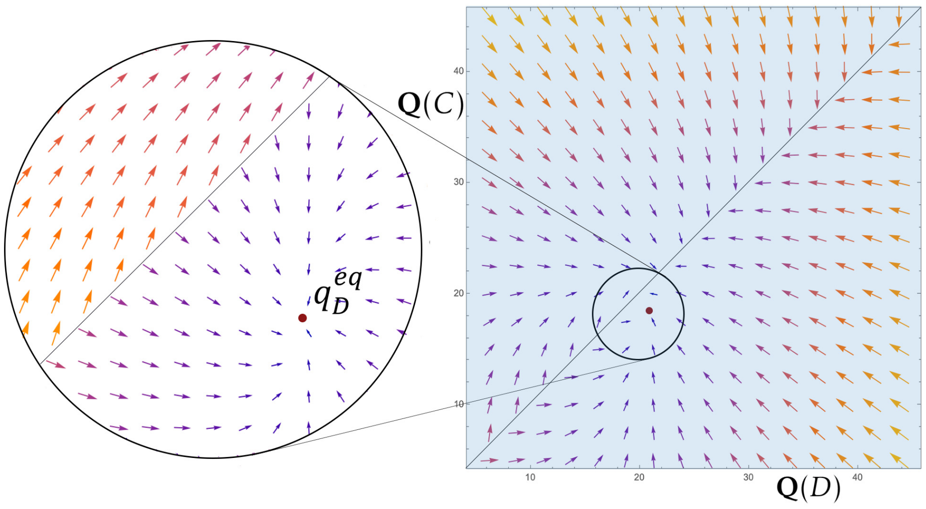

(b) Phase space with $g = 1.1$.

Figure 4: Stationary points are marked with a red dot. The domain of attraction of the cooperative outcome is green-shaded, and the one for the non-cooperative outcome is blue-shaded.

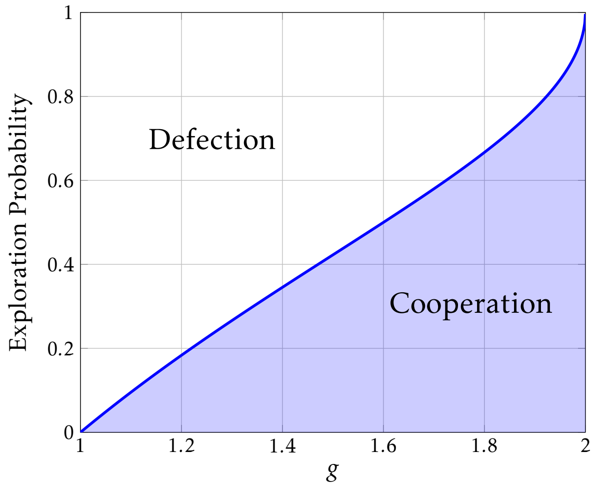

Figure 5: Maximum exploration rate $\underline{\varepsilon}$ to support the cooperative equilibrium, as a function of the growth rate. For all $\varepsilon > \underline{\varepsilon}(g)$ there does not exist a steady-state where both algorithms learn to cooperate.

adaptive agents play a symmetric profile of actions too often. We call this effect the *coordination bias*: the estimated value of action a is correct *conditional on the opponent playing (almost always) the same action*. Alice and Bob are *coupled*: their estimates tend to evolve symmetrically. When agents begins defecting, their experiments with cooperation are too infrequent, and their estimate of the value of cooperation remains biased. Effectively, Alice is too slow to realize the downside from cooperating when Bob defects, and the benefit of defecting when Bob cooperates.

The pseudo-steady-state on the boundary is the continuous-time counterpart of these cooperative cycles in the discrete system. The discrete cycles tend to a single point in the continuous-time limit. In the pseudo-steady-state, agents spend some "local time" playing cooperation: we interpret the weights $\tau, 1-\tau$ assigned to the fields on the boundary as the fraction of time dedicated to cooperation and defection, respectively.[5] The local time is such that the infinitesimal incentives around the stationary point are balanced.

Figure 6b plots this quantity and shows that the proportion of time spent playing the cooperative profile at equilibrium varies with g. Notice that the analytical local time spent cooperating approximates well the estimates from the simulations, even though the discrete system exhibits chaotic behavior.

[5]This intuition can be made formal using the idea of hysteresis loop around the boundary; see di Bernardo et al. (2008)

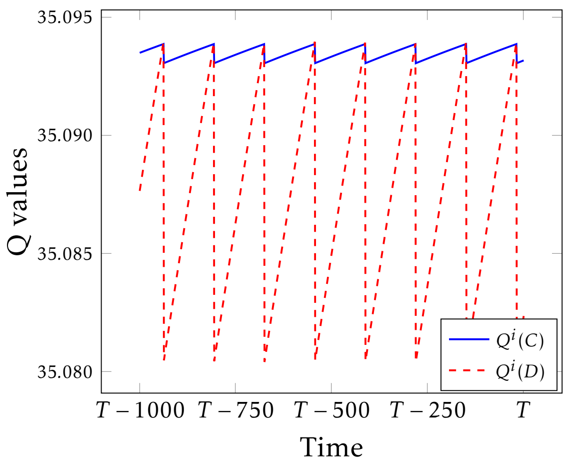

(a) Cycles of play around the cooperative equilibrium in the discretized ODE system.

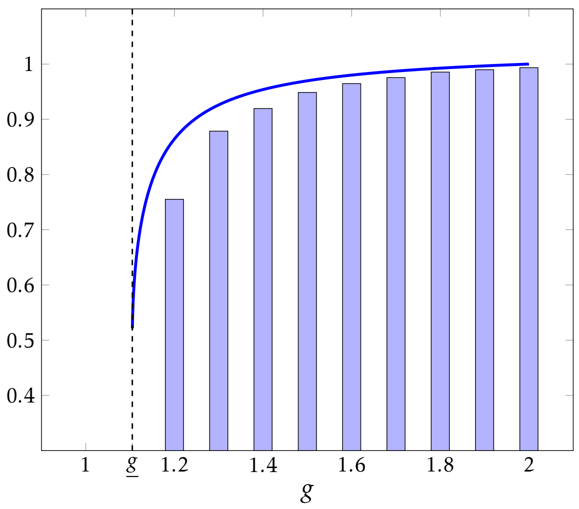

(b) Proportion of time spent playing the cooperative outcome in q_C^{eq}, analytically and in the simulations.

Figure 6

4 Main Results

The mechanics of coordination bias, identified in Section 3, appear tied to the policy of the reinforcer. We show that the driving force of inadvertent coupling lies in the algorithm's uneven learning rates across different actions. Learning at different rates about different actions leads to coordination bias. This negative result suggests a sufficient condition for avoiding inadvertent coupling: uniform learning rates across actions.

4.1 A Negative Result

The ε-greedy Q-learning analysis in the Prisoner's Dilemma of Section 3 brings out a mechanism which sustains collusive behavior between algorithms. Suppose Alice's preferred action is cooperation: at rate $1-\frac{\varepsilon}{2}$ she learns about the payoffs of cooperating, while she learns about the payoffs of defection more slowly, at rate $\frac{\varepsilon}{2}$. Exploration regulates how quickly Alice learns about the payoff of a deviation. Insufficient exploration impairs the ability of the algorithm to wash away existing bias — discovering the value of the dominant strategy becomes difficult. This phenomenon can be formalized without referring to a specific policy. In fact, a given policy only affects the learning rates α_a of different actions. For example, in the case of ε-greedy Q-learning, recall the differential equations within the maximal continuity domain $\omega_{D,D}$:

$$\begin{cases} \dfrac{d\mathbf{Q}_C^A}{dt}(t) = \quad \boldsymbol{\alpha}\dfrac{\boldsymbol{\varepsilon}}{\mathbf{2}} \quad \left[\left(1-\dfrac{\varepsilon}{2}\right)g + \dfrac{\varepsilon}{2}2g + (\gamma-1)\mathbf{Q}_C^A(t)\right] \\ \dfrac{d\mathbf{Q}_D^A}{dt}(t) = \boldsymbol{\alpha}\left(\mathbf{1}-\dfrac{\boldsymbol{\varepsilon}}{\mathbf{2}}\right)\left[\left(1-\dfrac{\varepsilon}{2}\right)2 + \dfrac{\varepsilon}{2}(2+g) + \gamma\mathbf{Q}_C^A(t) - \mathbf{Q}_D^A(t)\right] \end{cases}$$

In the language of separable reinforcers, the decision rule only affects $\alpha_a^i(\theta^i)$. When time is continuous, each estimate is updated according to its payoff given the opponents' actions — the only role of the policy is to determine the relative learning rates. It is clear from this discussion that the absolute magnitude of the learning rates does not matter, which is why we focus on the relative rates.

Definition 6. The relative learning rate of action a_i is the ratio

$$RLR(a_i) = \frac{\alpha_{a_i}}{\sum_{a\in A_i}\alpha_a}.$$

Theorem 2 shows how differences in RLR across actions generally give rise to the coordination bias. The coordination bias appears in a Prisoner's Dilemma for any pair of agents using any reinforcer. For simplicity, we restrict attention to reinforcers with maximal continuity domains equal to $\omega_{C,C}$ and $\omega_{D,D}$, and learning rates α_C, α_D constant over both.

Theorem 2. *Let each agent learn through the same greedy reinforcer in a Prisoner's Dilemma, and let Assumption S be satisfied. There exist an open set $A \subset \mathbb{R}_+^4$ such that for all parameters $\{\alpha_j(\omega_{k,k})\}_{j,k=C,D} \in A$ there exists a pseudo-steady-state on the boundary $\overline{\omega}_{C,C} \cap \overline{\omega}_{D,D}$.*

We prove Theorem 2 formally in the Appendix, but we provide a brief sketch of the proof here. The main idea is to construct a pseudo-steady-state of the reinforcer by mimicking the construction of the pseudo-steady-state we found in Section 3.1. That is, we want parameters such that the vector fields on the two sides of the boundary between maximal continuity domains are in equilibrium. To do so, we first deal with the case where the local time on the switching surface is equal on either side of the surface. We show that it is possible to construct a loop in $\mathbb{R}^2$ by varying the parameters α_C, α_D and the value θ^* on the boundary. We generate a homotopy between the loop and the origin by varying these parameters, thus showing that there exists a pseudo-steady-state. Adjusting the local time leads to continuous roto-translations of the homotopy, thus there must exist an open interval of α_C, α_D which generates a pseudo-equilibrium on the switching boundary.

The Theorem highlights an important fact: even in dominant-strategy-solvable games, reinforcers will not play the dominant strategy for various ranges of parameters.

4.2 Uniform Learning Respects Incentives

Unlike the Prisoner's Dilemma, in many situations dominant strategies also represent the desirable outcome, from the perspective of a market designer or an implementor. For example, an auctioneer who adopts a second-price auction hopes to recover the dominant-strategy outcome in order to maximize its profits.

We provide a simple condition that guarantees reinforcers converge on dominant strategies. Reinforcers' relative learning rates must be uniform across all actions. We will need the following technical assumption:

Assumption A3 (Thickness)**.** Let $G^t_{-i}(a)$ be the distribution over actions of all players but i at time t. Then, there exists a $\chi > 0$ and an T such that for all $t > T$, $G^t_{-i}(a) \geq \chi$ for all $a \in A_{-i}$.

Thickness ensures that sufficient exploration is carried out by all players in the limit. This requirement is easily satisfied by any algorithmic system which adopts a ε-greedy policy, for example. More generally, thickness states that each action profile is played with positive (albeit small) probability in the limit.

Theorem 3. *Suppose Assumption A3 is satisfied for all players. In any game with a dominant strategy equilibrium, a reinforcer with $RLR(a_i) = RLR(\tilde{a}_i)$ for all $a_i, \tilde{a}_i \in A_i$ learns the dominant strategy. If the forward limit set of θ is a singleton, then θ converges on the dominant strategy.*

This result is surprisingly powerful. In particular, we make almost no assumption about the opponent's play: as long as all actions are played with some positive probability even in the limit, the reinforcer will learn to play its dominant strategy. Compare this with the previous result, Theorem 2, which required symmetric reinforcers in a Prisoner's Dilemma. Uniform learning rates ensure any reinforcer will learn the dominant strategy for any number of opponents, as well as opponents who adopt different learning algorithms, or the same learning algorithm with different parameters. All these asymmetries can be accommodated by Theorem 3.

The assumption that relative learning rates be uniform across actions may appear stringent: it might for example require restricting the exploration of the algorithm to try each action uniformly at random. We propose instead a different interpretation of identical RLR across actions.

Consider again Q-learning. The algorithm updates the statistic of action a_i when action a_i is taken and its reward is observed, but it leaves other statistics unattended when the corresponding action is not selected. Suppose however that the agents were able to compute counterfactuals. That is, suppose that, after choosing an action a_i in period t, the algorithmic agent was able to work out $r_t(\tilde{a}_i, a_{-i})$ for all $\tilde{a}_i \neq a_i$. Then, the statistics of all actions could be updated simultaneously, using the reward that each action would have procured had it been played in that period. Simultaneous updates are sometimes referred to as *synchronous* learning:[6] in this case learning happens at the same rate for all actions. The ability to compute counterfactuals affects the learning rates: the second term in $\alpha_a^i \cdot (\pi_\varepsilon(\theta^i(t)))_a$ disappears when agents update synchronously. When asymmetric learning rates arise from missing or asymmetric experiments, counterfactual information (that is, a correct model of the environment) is sufficient to eliminate the asymmetry. The following corollary formalizes this intuition.

Corollary 2. *Under the same assumptions of Theorem 3, a reinforcer who can compute counterfactuals always learns the dominant strategy. If its forward limit set is a singleton, it converges to the dominant strategy.*

It is perhaps not surprising that counterfactuals help to learn to play equilibria. In fact, the theory of Nash equilibrium is based on the assumption that agents can compute the payoff that would have obtained if they had played a different action, treating the opponents' strategies as fixed. This in turn allows them to evaluate incentives to deviate. Corollary 2 establishes that reinforcer algorithms successfully rule out dominated strategies, provided they have access to a method to compute counterfactuals. Reinforcers with counterfactuals will learn to play the (unique) equilibrium.

More generally, let us consider the procedure of iterated elimination of strictly of dominated strategies (IESDS). However, we rescrict deletion to strategies strictly dominated by another *pure* strategy, because reinforcers do not deal well with mixed strategies.[7]

Definition 7. We say that an action $a_i \in A_i$ is *pure-rationalizable* if there is an order of IESDS such that a_i survives the IESDS procedure.

In general, for a certain order of deletion of dominated strategies action a_i might get eliminated. However, as long as there is an order such that a_i survives the IESDS process,

[6]The term synchronous appears in Asker et al. (2022), but the idea of agents learning from counterfactuals is present already in Tumer and Khani (2009).

[7]Definition 1 makes clear that it is impossible for adaptive algorithms to learn the value of randomizing across actions.

we consider a_i pure-rationalizable. Our next theorem shows that reinforcers with access to counterfactuals only play pure-rationalizable strategies in the limit.

Theorem 4. *Let all players in game G learn through a ε-greedy reinforcer with $RLR(a_i) = RLR(\tilde{a}_i)$ for all $a_i, \tilde{a}_i \in A_i$ for all $i \in N$. Assume $\varepsilon > 0$ is small enough so that the reward's order is preserved, i.e. if a_{-i} is the preferred profile of actions of agent i's opponent, $\mathbb{E}_{\pi_{-i}}[r(a_i, \pi_{-i})] > \mathbb{E}_{\pi_{-i}}[r(\tilde{a}_i, \pi_{-i})]$ when $r(a_i, a_{-i}) > r(\tilde{a}_i, a_{-i})$. Then, all actions learned by the players are pure-rationalizable in the game G under the same IESDS order.*

One implication of Theorem 4 is that in a supermodular game ε-greedy reinforcers will learn rationalizable strategies. If the equilibrium is unique, then algorithms will always learn the unique equilibrium. In any pure-dominance-solvable game, reinforcers will learn the pure-strategy Nash equilibrium.

We can interpret relative learning rates in an intuitive sense as the relative ability to work out counterfactuals for a given action. Because the utility of a given action depends on the opponent's path of play, unever learning rates generate biased estimates. Small relative learning rates fail to account for asymmetric play, impairing the ability of the algorithm to best-respond. Uniform learning rates instead guarantee correct counterfactual estimates. With unbiased counterfactuals, abandoning dominated strategies is immediate.

In the next section, we leverage these results for implementation in hybrid markets: games played by rational as well as learning agents. Furthermore, Sections 6.2 and 6.3 show how Theorems 3 and 4 can be applied to study analytically environments that received considerable attention in the experimental literature.

5 Application: Learning-Robust Mechanism Design

In this section, we develop an application of the results about relative learning rates. We consider the problem of implementation of social choice functions. While strategy-proof implementation is the standard required by rational implementation, guaranteeing robustness of implementation to the presence of adaptive, learning agents, requires further considerations. In Section 4 we saw how traditional strategy-proof implementation is vulnerable to the inadvertent coupling of adaptive agents that prevents convergence on dominant strategies. In this section, we apply Theorem 3 to overcome this vulnerability and guarantee learning-robust implementation.

5.1 Model

We consider the basic setting of Dasgupta et al. (1979). Let $\mathcal{X}$ be the set of possible outcomes, and let there be n agents with types $(\lambda_i)_{i=1,\dots,n} \in \bigtimes_{i=1\dots n} \Lambda_i = \Lambda$. Type λ_i determines agent i's preferences $u_i\colon \mathcal{X} \times \Lambda_i \to \mathbb{R}$ over outcomes. A social choice rule (SCR) is a function $f\colon \Lambda \to \mathcal{X}$, that specifies an outcome for each type profile. Adopting the usual revelation principle, the designer chooses a direct mechanism $g\colon \Lambda \to \mathcal{X}$ such that it assigns an outcome to each possible report of the agents. We say a SCR f is implementable if (i) the set of equilibria $\mathcal{E}_g(\lambda)$ of the game described by g is non-empty for all type profiles λ; and (ii) $g(\mathcal{E}_g(\lambda)) = f(\lambda)$.

The seminal result of Dasgupta et al. (1979) relates Nash implementation with strategy-proof implementation: as long as the domain of preferences of the players is rich, the two concepts are equivalent. We thus focus on strategy-proof (or dominant-strategy, or straightforward) implementation of a SCR f. That is, we are looking for a direct mechanism such that truth-telling is a dominant strategy. Equivalently, f is straightforwardly implementable if

$$u_i(f(\lambda_i, \lambda_{-i}), \lambda_i) \geq u_i(f(\eta_i, \lambda_{-i}), \lambda_i) \qquad \forall \eta_i \neq \lambda_i.$$

Dasgupta et al. (1979) provide the following characterization of dominant-strategy implementable social choice rules:

Theorem (4.3.1)**.** *An SCR is truthfully implementable in dominant strategies if and only if it is independently person-by-person monotonic (IPM).*

We depart from the standard setting described so far in two important ways. First, we assume that a subgroup of agents $L \subseteq N$ each act according to the choices of their own reinforcer. Learning requires repeated interaction with the environment, therefore our second point of departure from the standard implementation setup is the repetition of the implementation problem. However, we want to avoid incentives arising from repeated interactions, as well as manipulation of the algorithms by forward-looking participants. For this reason, we assume that the subset of rational agents $R = N \setminus L$ is short-lived or myopic. In each period a fresh group of rational agents arrives and both rational and learning agents choose a report. The implementor then selects the outcome according to the mechanism she selected, payoffs are realized and rational agents leave the game. We call this setting a *hybrid* implementation problem because rational and learning agents coexist.

When adopting a truthful strategy-proof mechanism in a hybrid problem, rational agents will report truthfully. Will reinforcers learn to play the dominant strategy? As seen in Section 3, algorithmic agents may never do. Instead, they may collude together to obtain higher individual payoffs, in spite of the implementor's goals. We thus seek learning-robust truthful mechanisms.

Definition 8. A SCR is *learning-robust* truthfully implementable if:

- Rational agents play truthfully (i.e. report $\lambda_{\text{truthful}}$), and
- Reinforcers learn the truthful report $\lambda_{\text{truthful}}$ uniquely.

We say a mechanism is learning-robust if it learning-robust truthfully implements a given SCR.

In a learning-robust mechanism, adaptive agents will learn that reporting truthfully provides the largest value. The actions taken by the reinforcers might be tainted by exploratory policies, but the estimates they identify will agree with the strategy-proof nature of the game.

5.2 Feedback Design

In Parkes (2004) the author argues that mechanism design can play an important role in shaping algorithmic systems. The focus of that work is mainly on how to improve learning speed and how to select the designer's preferred equilibrium when decision-makers are algorithms. Parkes describes *learnable* mechanism design, the idea of explicitly designing mechanisms to maximize and improve performance considering the agent's adaptive behavior. As he suggests, *"a useful learnable mechanism would provide information, for example via price signals, to maximize the effectiveness with which individual agents can learn equilibrium strategies"*. Here we formalize this intuition, and we show that feedback design can make traditional strategyproof settings robust to adaptive algorithmic players.

We do so leveraging our results, which guarantee that equilibrium is restored provided counterfactuals can be computed. Supplying enough information so that algorithms can evaluate counterfactual returns falls onto the mechanism designer. In this imperfect information setting, counterfactual calculations depend critically on the opponents' private information. The designer, who elicits all private information, must partly reveal it ex-post. We refer to this ex-post revelation as a feedback provision.

Definition 9. A *feedback statistic* for mechanism f is a factorization of f through partitions. It is composed of the following elements:

- A *signal space* S, which is a partition of Θ_{-i};
- A map $\phi_i \colon \Theta_{-i} \to S$;
- A map $g \colon \Theta_i \times S \to \mathcal{X}$;

such that

- The diagram commutes, i.e. $f(\theta_i, \theta_{-i}) = g(\theta_i, \phi_i(\theta_{-i}))$ for all θ_i, θ_{-i};
- The map ϕ_i is a partition map, i.e. $\phi_i(\theta_i) \ni \theta_i$.

We denote a feedback statistic by its map ϕ_i. A collection $(\phi_i)_i$ of feedback statistics for each agent i is a *feedback structure*.

A feedback statistic determines the amount of information communicated by the designer *after* the outcome is realized. By accessing ex-post information, the algorithms can now compute counterfactuals: feedback statistics fully reveal what would have happened had a player submit a different report.

Proposition 3. *Under Assumption A3, a mechanism f augmented with feedback structure $(\phi_i)_i$ is* learning-robust *if:*

- *f is an independently person-by-person monotonic SCR; and*
- *$(\phi_i)_i$ is a feedback structure for mechanism f.*

The proof follows from Corollary 2. Notice that there always exists a learning-robust mechanism: it is one where each feedback statistic communicates all opponent's types truthfully.

Corollary 3. *Any SCR f which satisfies IPM is learning-robust truthfully implementable. A learning-robust mechanism which implements f is simply $(f, (\phi_i)_i)$ with $\phi_i \colon \Theta_{-i} \to \Theta_{-i}$ the identity map for all $i = 1, \ldots, n$.*

This robust implementation relies on full revelation: the designer does not hide anything from the participants in the mechanism. However, the full-revelation feedback structure might have some drawbacks. For example, full revelation might not be desirable, particularly when the implementation problem is repeated. Communicating all types also results in large communication complexity, and potentially high computational burden on the agents themselves, who need to re-compute the mechanism's allocation for each possible report. To formalize the desire for reduced communication, we define a partial order on feedback statistics:

Definition 10. Feedback statistic ϕ_i is *more private* than feedback statistic ψ_i, denoted $\phi_i \trianglerighteq \psi_i$, if $\phi_i(\theta_{-i}) \supseteq \psi_i(\theta_{-i})$ for all θ_{-i}.

Any two type profiles that are indistinguishable under a less private rule should be indistinguishable under a more private rule. As mentioned, the privacy order is a weak partial order: not all feedback statistics are comparable. However, it turns out that under the privacy order maximum and minimum are well-defined: the feedback statistics together with the privacy order form a lattice.

Proposition 4. *Feedback statistics together with the privacy order form a complete lattice.*

Proof. We simply need to show that for any two elements ϕ_i, ψ_i there exist a join $\phi_i \vee \psi_i$ and a meet $\phi_i \wedge \psi_i$ which satisfy the feedback statistic definition. The argument follows from the lattice structure of the set of partitions with the partial order *coarser-than*. Note that $\phi_i^{-1}(\{x\colon x \in \Theta_{-i}\})$ defines a partition of the space Θ_{-i}, and the same is true for the ψ_i. We then require the preimage of join $(\phi_i \vee \psi_i)$ to be the finest partition which is coarser than both the preimages of ϕ_i and ψ_i. Formally, let $A \subset \phi_i^{-1}(\{x\colon x \in \Theta_{-i}\}) \vee_P \psi_i^{-1}(\{x\colon x \in \Theta_{-i}\})$, then

$$(\phi_i \vee \psi_i)(\theta_{-i}) = (\phi_i \vee \psi_i)(\theta'_{-i}) \text{ for all } \theta_{-i}, \theta'_{-i} \in A$$

Similarly, define the meet as the function $\phi_i \wedge \psi_i$ such that it is constant over the meet of the two partitions. Again, let $B \subset \phi_i^{-1}(\{x\colon x \in \Theta_{-i}\}) \wedge_P \psi_i^{-1}(\{x\colon x \in \Theta_{-i}\})$, then

$$(\phi_i \wedge \psi_i)(\theta_{-i}) = (\phi_i \wedge \psi_i)(\theta'_{-i}) \text{ for all } \theta_{-i}, \theta'_{-i} \in B$$

The completeness of the lattice structure descends directly from the completeness of the partition lattice. □

From Proposition 4 it follows that there exist both a minimally- and a maximally-private feedback statistic. The minimally-private statistic is the full-revelation feedback statistic: it reveals all information, and it is clearly less private than any other feedback statistic. The maximally-private rule instead is interesting from the perspective of the market designer.

We observe another interesting property of the privacy order that stems from its connection with the set of partitions of the power set of Θ_{-i}:

Corollary 4. *The communication complexity of a feedback statistic is monotonically decreasing in the privacy order.*

The maximally private feedback statistic is highly desirable: it has the lowest communication complexity and it maintains the highest level of privacy while supporting truthful implementation. We say a learning-robust mechanism is optimal if it robustly implements the SCR f and it does so with maximal privacy (and consequently, minimal communication cost) for all agents.[8] Next, we derive the maximally private feedback statistic in the setting of efficient implementation with transferable quasi-linear utility.

5.3 Maximally Private Learning-Robust VCG

In this setting let $v_i(x)$ be the value of agent i for outcome x, and assume quasi-linearity in transfers. The goal of the designer is to select the allocation x^* such that

$$x^* = \operatorname*{argmax}_{x \in \mathcal{X}} \sum_{i=1}^{n} v_i(x).$$

Again we focus on truthful reporting mechanisms. One mechanism available to the designer is the well-known VCG mechanism. In particular, the mechanism with the Clarke pivot rule selects the optimal allocation for the given reports and assigns payments for agent i equal to

$$p_i = \sum_{j \neq i} v_j(x^*) - \max_{x \in \mathcal{X}} \sum_{j \neq i} v_j(x).$$

Given these payments, rational agents are incentivized to report truthfully: reporting their true values is a dominant strategy. In order to ensure implementation for an algorithmic system, however, we need to augment VCG with an appropriate feedback structure. The feedback from the traditional VCG is rather limited: with only the knowledge of the price for the implemented outcome, counterfactual returns for other actions are impossible to compute. We define a learnable mechanism, pVCG, and we show that its feedback structure is maximally private.

Definition 11. A pVCG mechanism is a pair of mechanism and feedback structure, such that:

- The allocation and payment function correspond to the VCG allocations and payments; and

[8]Note that we defined the privacy lattice for feedback statistics, not for feedback structures. When we analyze feedback structures, we implicitly consider the product lattice on the product space of feedback statistics. This is correct because we assume private communication, but the analysis would likely change if we allowed public communication.

- The feedback structure communicates to each agent a vector of personalized prices $(p_i(x))_{x\in\mathcal{X}}$, defined as
$$p_i(x) = \sum_{j\neq i} v_j(x) - \max_{x'\in\mathcal{X}} \sum_{j\neq i} v_j(x').$$

Intuitively, a pVCG mechanism provides each algorithmic player with personalized prices for all possible outcomes that could have been implemented. This menu aggregates the information about other player's valuations and allows to compute counterfactuals. Note that a player's feedback structure does not depend on that player's report. Therefore, each $p_i(x)$ is independent of the vector of reported $(v_i(x))_{x\in\mathcal{X}}$.

Proposition 5. *The pVCG mechanism implements the social optimum even when players bid through greedy adaptive agents.*

Proof. It suffices to show that each algorithm can compute its counterfactual return from reporting any vector $(\hat{v}_i(x))_{x\in\mathcal{X}}$. For any report $(\hat{v}_i(x))_{x\in\mathcal{X}}$, the player can compute which outcome $\hat{x}$ would have been implemented:

$$\hat{x} = \operatorname*{argmax}_{x\in\mathcal{X}} \hat{v}_i(x) + p_i(x)$$

Fixed the other player's reports, $p_i(x)$ represents the sum of other players' valuations for outcome x, up to a constant. It is then easy to compute the counterfactual return for reporting $(\hat{v}_i(x))_{x\in\mathcal{X}}$: player i would obtain $v_i(\hat{x}) + p_i(\hat{x})$. Now, because VCG is a strategy-proof mechanism, Proposition 3 applies and adaptive algorithms learn to play truthfully, thus implementing the social optimum. $\square$

The feedback structure of pVCG is maximally private: for any coarser partition of the outcome space it is a simple exercise to produce a valuation for which the counterfactual is not uniquely determined. Thus, pVCG is the optimal learning-robust VCG mechanism.

Notice how in a second-price auction for a single item, the pVCG mechanism reduces to providing the lowest-bid-to-win to all the losers. Anecdotally, this practice is becoming more common in online auctions, even in games that do not have a dominant strategy (but can be solved by iterated elimination), as pointed out in Banchio and Skrzypacz (2022).

We offer a simple price-theoretic interpretation of pVCG in a unit-demand model with multiple goods for sale.

Example 2. *Assume that the auctioneer is selling goods $x_1,\ldots,x_k$ to agents $1,\ldots,n$ optimally. The pVCG mechanism requires each agent to communicate their values for each good to the auctioneer. After this communication, each agent is offered a personalized menu: the agent* *could purchase any goods at the price specified in the menu. Clearly consumers choose the good that maximizes their utility subject to the unit-demand constraint. In addition to consuming their favorite good, they can also infer the utility they could have obtained had they selected a different allocation: the menu provides prices for all goods $x_1, \ldots, x_k$. Thus, even adaptive agents would converge on the dominant strategy, by means of counterfactuals evaluations.*

In this example, the feedback of pVCG is an aggregator of market information, which helps agents evaluating the true value of truthful reporting. As suggested by Parkes (2004), price signals serve as learning aids to individual adaptive agents.

6 Extensions

In this section we extend our analytic characterization, and we better position our results vis-a-vis the literature on algorithmic collusion by applying the arguments of Section 4 to two recent papers by Asker et al. (2022) and by Banchio and Skrzypacz (2022).

6.1 General Prisoner's Dilemma

Of course, the contribution game of Section 3 can be seen as a particular one-dimensional parametrization of the Prisoner's Dilemma. A complete parametrization of the incentives in a Prisoner's Dilemma is given in Friedman and Oprea (2012) and reproposed in Figure 7a. We normalize the cooperation payoff to 1 and the sucker's payoff to 0, while we vary the payoff to deviation x and the payoff to mutual defection y.

We can replicate the analysis carried out for the contribution game in this more general setting, and we reach similar conclusions.

Proposition 6. *There always exists a steady-state $q_D^{eq} \in \omega_{D,D}$. Moreover, there exists a pseudo-steady-state $q_C^{eq} \in \overline{\omega}_{D,D} \cap \overline{\omega}_{C,C}$ only when the following conditions are satisfied:*

$$\begin{cases} 1 < x < \frac{4+2\varepsilon-\varepsilon^2}{2\varepsilon-\varepsilon^2} - 4\sqrt{\frac{1}{2\varepsilon-\varepsilon^2}}, \\ 0 \leq y \leq -4\sqrt{\frac{(\varepsilon-2)^2\varepsilon^2[\varepsilon^2(x-2)-2\varepsilon(x-2)+4(x-1)]}{(4-2\varepsilon+\varepsilon^2)^4}} + \frac{16-4\varepsilon^3(x-1)+\varepsilon^4(x-1)-8\varepsilon(x+2)+4\varepsilon^2(1+2x)}{(4-2\varepsilon+\varepsilon^2)^2} \end{cases}$$

The conditions for existence of a pseudo-steady-state appear complex, but the visualization in Figure 7b helps disentangling the various forces at play.

The higher the exploration rate, the more extreme the parameters x, y need to be to sustain the cooperative equilibrium. When both x and y are large the payoff from mutual defection is close to mutual cooperation, and a one-period defection provides large

		Bob	
		C	D
Alice	C	$1,1$	$0,x$
	D	$x,0$	y,y

(a) Payoffs of the stage game. $1 < x < 2$, $0 < y < 1$.

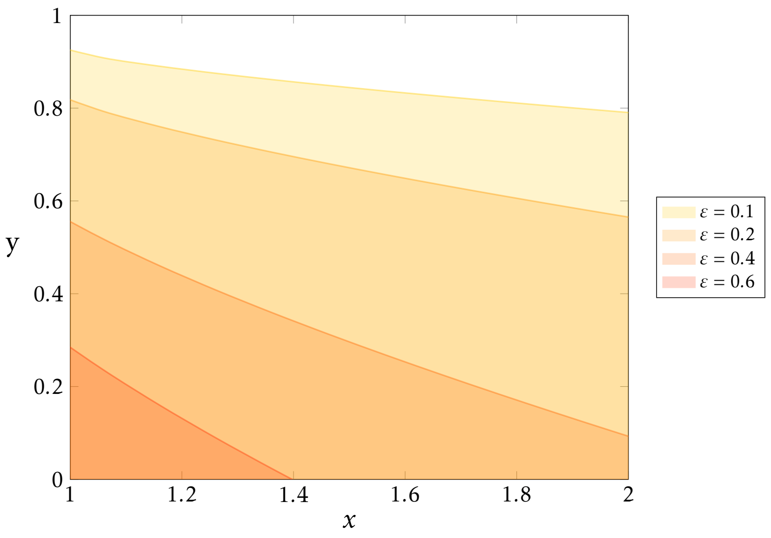

(b) Existence of cooperative pseudo-steady-state in the Prisoner's Dilemma parameter space.

Figure 7

unilateral benefits. These are the cases providing the strongest incentives for defection, while when both x and y are low the opposite is true. The Figure clearly reflects these intuitions for various levels of exploration.

6.2 Bertrand Competition

Consider the setting of Asker et al. (2022). The authors simulate algorithmic competition in a Bertrand oligopoly, and find that collusion depends critically on the synchronicity of the algorithm. We show that their results can be derived analytically, and how competition is enforced only when players have access to counterfactuals with respect to their pricing decisions.

There are two firms, Alice Inc. and Bob Ltd., which face a common demand for their product. For a simple illustrative model, we assume that the market demand is $D(p_A, p_B) = 3 - \min\{p_A, p_B\}$, and if the two firms charge the same price they split demand equally. Suppose that each firm has 0 marginal cost, and for simplicity let the firms choose only between two prices: $p \in \{0.5, 2\}$. Profits equal price times individual demand. This Bertrand game has only one static Nash equilibrium: the profile $\{0.5, 0.5\}$. Asker et al. (2022) consider two variations of the Q-learning algorithm, both of which are *greedy*, i.e., the action taken is always the one with the highest estimated value.

(i) Asynchronous Greedy Q-learning: the algorithm updates only the Q-value of the action taken in each period;

(ii) Synchronous Greedy Q-learning: the algorithm updates all Q-values in each period, with the return that he could have obtained had he played the other action instead, but holding the opponent's action fixed.

We plot both systems in Figure 8 for $\gamma = 0$.[9] The figures depict the vector fields governing the dynamics of the continuous-time analogous of each Q-learning procedure, with the value of the competitive price on the vertical axis and that of the collusive price on the horizontal axis.

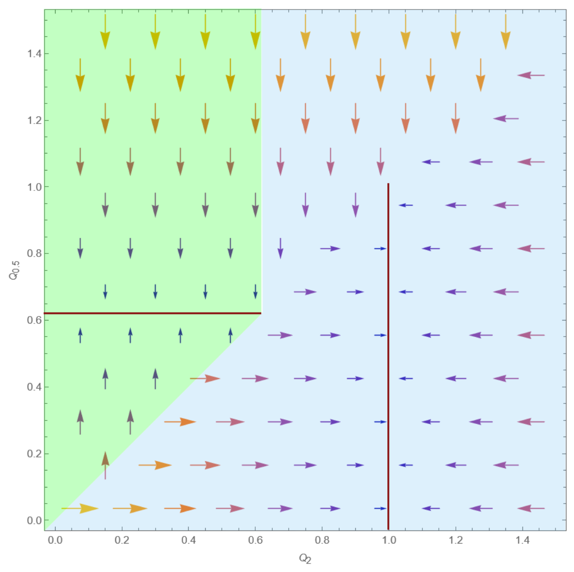

(a) Asynchronous updating.

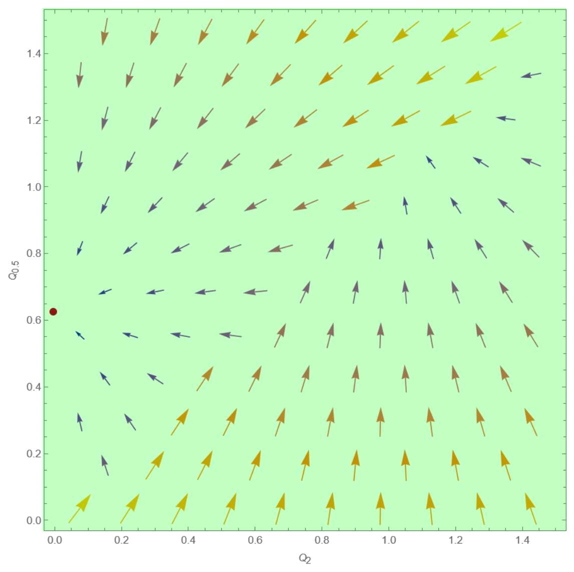

(b) Synchronous updating.

Figure 8: The green-shaded area denotes the domain of attraction of the competitive outcome, while the blue-shaded area is the domain of attraction of the collusive outcome. The red dot and red lines are the equilibria of the systems.

Asynchronous Learning. The fields when both firms play asynchronous Q-learning and both choose 0.5 and 2, respectively, are:

$$\begin{cases} \frac{d\mathbf{Q}_{0.5}}{dt} = \alpha\left(\frac{5}{8} + (\gamma - 1)\mathbf{Q}_{0.5}\right) \\ \frac{d\mathbf{Q}_2}{dt} = 0 \end{cases} \quad \text{on } \omega_{0.5,0.5} \qquad \begin{cases} \frac{d\mathbf{Q}_{0.5}}{dt} = 0 \\ \frac{d\mathbf{Q}_2}{dt} = \alpha\left(1 + (\gamma - 1)\mathbf{Q}_2\right) \end{cases} \quad \text{on } \omega_{2,2}$$

[9]The choice of $\gamma = 0$ reflects the specification of Asker et al. (2022), but we provide the vector fields for general values of γ, and notice that the same intuitions apply.

Figure 8a plots the fields within their domains. As shown in the picture, there are two equilibrium regions. For values of $\mathbf{Q}_2 \leq \mathbf{Q}_{0.5} = \frac{5}{8}$ the algorithms converge on the competitive outcome. However, for $\mathbf{Q}_{0.5} \leq \mathbf{Q}_2 = 1$ the algorithms collude. Notice also that the domains of attraction of these equilibria are profoundly unbalanced: in order to converge on competition, Q-learning needs to be initialized with a strong bias towards competition. Otherwise, the collusive outcome is an attractor. In particular, the optimistic initialization used in Asker et al. (2022) and common in the literature leads to collusive outcomes.

These results are robust to an ε−greedy specification: the *coordination bias* introduced in Section 3 again sustains collusion. Because most observations of the returns from a supra-competitive price are obtained when colluding, the estimates of returns from charging a price of 2 are biased during a competitive phase. The persistence of this bias amounts to insufficient exploration of alternative strategies.

Synchronous Learning. Instead, if both firms adopt Synchronous Q-learning, the system is described by the following fields:

$$\begin{cases} \frac{d\mathbf{Q}_{0.5}}{dt} = \alpha\left(\frac{5}{8} + (\gamma - 1)\mathbf{Q}_{0.5}\right) \\ \frac{d\mathbf{Q}_2}{dt} = \alpha\left(\gamma \mathbf{Q}_{0.5} - \mathbf{Q}_2\right) \end{cases} \text{on } \omega_{0.5,0.5} \qquad \begin{cases} \frac{d\mathbf{Q}_{0.5}}{dt} = \alpha\left(\frac{5}{4} + \gamma \mathbf{Q}_2 - \mathbf{Q}_{0.5}\right) \\ \frac{d\mathbf{Q}_2}{dt} = \alpha\left(1 + (\gamma - 1)\mathbf{Q}_2\right) \end{cases} \text{on } \omega_{2,2}$$

There is only one equilibrium, at $\mathbf{Q}_{0.5} = \frac{5}{8}, \mathbf{Q}_2 = 0$. The plot of Figure 8b shows a clear pattern: the two firms can only converge on competition. There is no sliding along the boundary between the competitive and collusive pricing: everywhere the trajectories move from colluding to competing. When the two firms are colluding, all arrows point upward: the intuition is that they overestimate the value of undercutting the opponent, because they do not internalize the effect that defecting from a collusive outcome will have on returns in the future. The counterfactual rewards do not account for the losses that will stem from a change in equilibrium. Once the firms start competing it is then impossible to revert back to collusion: the counterfactual return of a deviation is zero. Observe the contrast with the asynchronous case, where once agents begin to compete, they almost immediately revert back to collusion. The bias present in the asynchronous algorithm disappears in the synchronous version: actions are updated according to counterfactual returns, therefore the value of joint collusion is short-lived after competition begins. These result are not surprising, as Theorem 3 proves that collusion is unsustainable in a dominant-strategy game.

General Bertrand. The simple model above reduces the Bertrand game to a dominant-strategy game. It is a convenient simplification for the purposes of inspecting and plotting the dynamical systems, but the theory developed in Section 4 allows us to deal with much more general models.

Take for example the full model from Asker et al. (2022). Alice Inc. and Bob Ltd. have now constant marginal costs $c_A = c_B = 2$. They sell homogeneous goods and compete by setting prices. The set of feasible prices is composed of 100 equally spaced numbers between 0.01 and 10, inclusive. The set of prices is denoted by $P = \{p^1, \ldots, p^{100}\}$. Consumers buy from the firm with the lowest price, and demand is parametrized as

$$d_i(p_i, p_{-i}) = \begin{cases} 1 \text{ if } p_i < p_{-i} \text{ and } p_i \leq 10 \\ 1 \text{ if } p_i = p_{-i} \text{ and } p_i \leq 10 \\ 0 \text{ otherwise} \end{cases}$$

As the authors note, there are two Nash equilibria of this game, one (E_1) with $p_A = p_B = 2.0282$ and one (E_2) with $p_A = p_B = 2.1291$. The multiplicity is a consequence of the discretization of the space in equally spaced prices.

Proposition 7. *In a Bertrand oligopoly, if Alice Inc. and Bob Ltd. adopt any greedy reinforcers such that the relative speed of learning is the same across all prices, they either converge on E_1 or E_2.*

Proof. The proof of this proposition consists of verifying the assumptions of Theorem 4. As discussed earlier, Q-learning is a reinforcer, and ε-greedy policies guarantee that Assumption A3 is satisfied. By applying iterated elimination of strictly dominant strategies, only one of two pairs of prices can survive. Those pairs are exactly the equilibrium pairs. □

In particular, this result shows that the parameters of the algorithms are irrelevant for the convergence result. How fast the equilibria are reached will depend on the different discounting or learning rates, but convergence on an equilibrium is guaranteed.

6.3 First-Price Auction

Consider now the setting of Banchio and Skrzypacz (2022). The authors simulate algorithmic competition in an auction environment, and they find that revenues in First and Second Price Auction are substantially different when Q-learning algorithms choose bids. While the Second Price Auction appears to be competitive, the first-price auction is prone to collusion. Additionally, they find that providing counterfactuals in the first-price auction restores competition.

First, we propose an interpretation of their findings in light of our results. Let us consider the same model, where Alice.com and Bob.net bid in a First- (Second-) Price Auction for display advertising. Both have value of \$1 for the impression being auctioned, and they have access to a set of 19 equally-spaced bids $b_i \in \{0.05, 0.1, \dots, 0.95\}$. Banchio and Skrzypacz (2022) finds that, when the exploration parameter ε is held constant, the Second Price Auction (SPA) converges on the dominant-strategy equilibrium. In the First Price Auction (FPA) instead the bidders cycle between collusive pairs, interspersed with short "punitive" phases.

We interpret the cycling between collusive pairs as a form of sliding. To this end, consider the following simpler model, where Alice.com and Bob.net each have access only to two bids. The low bid is 0.1, while the high bid is denoted by x and varies in $[0.1, 0.55]$. Under these assumptions, both games are one-dimensional parametrizations of a Prisoner's Dilemma, and can therefore be mapped to the description of Proposition 6. Figures 9a and 9b show the payoff matrix for both game formats, while Figure 9c plots the parametric region where a collusive equilibrium exists, for both FPA and SPA.

Importantly, we observe that parameters such that a pseudo-steady-state exists for a SPA also generate a pseudo-steady-state for the FPA. The payment rules of FPA and SPA parametrize the Prisoner's Dilemma differently, and in such a way that FPA facilitates collusion through coupling and coordination bias.

A further result of that paper shows that by providing counterfactual information to Alice.com and Bob.net the designer restores competition in the First Price Auction. Note that the FPA with 19 admissible bids has two equilibria: one (E_1) sees both Alice.com and Bob.net bidding $b_A = b_B = 0.95$, and one (E_2) sees them bidding $b_A = b_B = 0.9$. Again, we can show:

Proposition 8. *In a first-price auction, if Alice.com and Bob.net adopt any greedy reinforcers with same relative speed of learning across bids, they converge on either E_1 or E_2.*

The proof is identical to that of Proposition 7 and is therefore omitted. In fact, first-price auctions and homogeneous Bertrand oligopolies are strategically equivalent. Banchio and Skrzypacz (2022) argues that the minimum-bid-to-win feedback Google provides in its FPA improves convergence and guarantees more competitive outcomes. The latter can be seen clearly in our framework, both in Proposition 8 as well as in the implementation problem we presented in Section 5: feedback restores the level-k reasoning which in turn guarantees successful implementation.

		Bob	
		0.1	x
Alice	0.1	$0.45, 0.45$	$0, \mathbf{1-x}$
	x	$\mathbf{1-x}, 0$	$\frac{1-x}{2}, \frac{1-x}{2}$

(a) Payoffs of the FPA.

		Bob	
		0.1	x
Alice	0.1	$0.45, 0.45$	$0, \mathbf{0.9}$
	x	$\mathbf{0.9}, 0$	$\frac{1-x}{2}, \frac{1-x}{2}$

(b) Payoffs of the SPA.

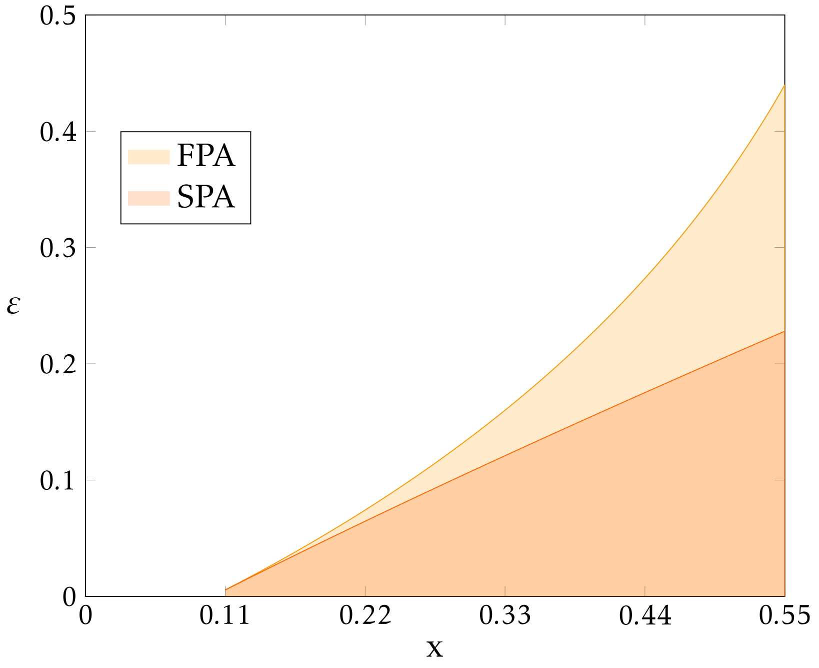

(c) Region of the parameter space such that a pseudo-steady-state exists for FPA and SPA, respectively.

Figure 9

7 Conclusion

This paper analyses collusion in games played by online learning algorithms. We take a theoretical perspective and, moving from burgeoning empirical and numerical evidence, we identify the drivers of collusive behaviour in a widely studied class of games. In particular, we first address the issue of the analytical intractability of strategic interaction among algorithms by showing they can be approximated with a system of ODEs. Then we apply this framework to dominant-strategy games, and prove that (ε-)greedy algorithms can learn to collude. We identify the mechanism sustaining collusion in the *coordination bias*: when algorithms realize the benefit of the dominant action too slowly, joint collusion appears more attractive. Involuntary coupling yields self-fulfilling biases in the estimates. We demonstrate this intuition in a Prisoner's Dilemma with Q-learning agents. We expect the techniques developed to analyze the simple Prisoner's Dilemma to yield insight in games with more complex strategic structure. In particular, we believe similar techniques could help in understanding how AIs reach tit-for-tat strategies when given monitoring technology. As an example of the power of our method, we apply the techniques to simple auctions in the spirit of Banchio and Skrzypacz (2022), where the same mechanism generates different results across payment rules.

We show that convergence on the dominant action is instead guaranteed for greedy algorithms if learning occurs at uniform rates for all actions. Algorithms that evaluate counterfactual rewards from actions not taken learn simultaneously for all actions, and thus converge on dominant strategies. The involuntary coupling at the heart of collusion may appear whenever learning rates are not uniform — differential learning rates is akin to oversampling bias.

Following these results, we design learning-robust mechanisms, which guarantee implementation in hybrid models where rational and learning agents coexist. Learning-robustness is guaranteed by a new layer in the mechanism design: ex-post feedback provision. We apply the hybrid implementation theory to design a mechanism, *pVCG*, that implements the social optimum in dominant strategies. pVCG provides personalized prices for all outcomes, aggregating the necessary information efficiently and allowing counterfactual evaluations for any report. We suspect that these design ideas could be successfully applied to settings with regret-minimizing agents, as additional feedback simplifies regret evaluations. Finally, we validate our theoretical results by analyzing the Bertrand oligopoly introduced in Asker et al. (2022), where our framework delivers an analysis of the driving forces while recovering their experimental results.

We view our paper as contributing to the growing literature studying strategic interaction of algorithmic agents. Algorithms shape the dimensions of rationality of these decision makers, and allow us to carry out a disciplined analysis of equilibria and market design for such boundedly-rational agents. Our work provides a theoretical analysis of collusion in games played by online learning algorithms. In doing so we prove a continuous-time approximation technique that can be applied more generally to the study of systems otherwise deemed intractable. We hope that this work will stimulate further analysis of the strategic interaction of learning algorithms. We focused on dominant strategy games, which intrinsically make collusion the hardest to sustain: the outcomes of games where the separation between competition and collusion is less stark remains unclear, and worthwhile to pursue. Our algorithms interact with the environment and adapt according to the feedback they receive, but many deployed market algorithms are instead trained offline. Our analysis points to coordination as a key driver of collusion, thus suggesting that offline algorithms may be less prone to collusive behavior.

We focused on implementation with myopic rational participants, but an interesting question is what could a sophisticated player achieve when competing against an automated decision-maker. The manipulability of these algorithms deserves further analysis, and we believe a setting similar to the one offered in this work could prove helpful in understanding these questions. Finally, algorithmic decision-making can be seen as a form of bounded rationality. This implies that the set of implementable outcomes is, in general, wider than that of rational agents. Theorem 4 suggests that arguments similar to Abreu and Matsushima (1992) could prove useful in enlarging the set of implementable outcomes; characterizing the set of implementable outcomes for purely adaptive decision makers is beyond the scope of this paper, but of independent interest.

References

Abreu, D. and H. Matsushima (1992): "Virtual implementation in iteratively undominated strategies: complete information," *Econometrica*, 993–1008.

Aouad, A. and A. Van den Boer (2021): "Algorithmic Collusion in Assortment Games," Working paper.

Asker, J., C. Fershtman, and A. Pakes (2022): "Artificial Intelligence, Algorithm Design and Pricing," *American Economic Review, P&P*, forthcoming.

Assad, S., R. Clark, D. Ershov, and L. Xu (2021): "Algorithmic Pricing and Competition: Empirical Evidence from the German Retail Gasoline Market," Working paper.

Banchio, M. and A. Skrzypacz (2022): "Artificial Intelligence and Auction Design," Working paper.

Benaim, M. (1996): "A Dynamical System Approach to Stochastic Approximations," *SIAM Journal of Control and Optimization*, 34, 437–472.

Brown, Z. Y. and A. MacKay (2021): "Competition in Pricing Algorithms," *American Economic Journal: Microeconomics*, forthcoming.

Börgers, T. and R. Sarin (1997): "Learning Through Reinforcement and Replicator Dynamics," *Journal of Economic Theory*, 77, 1–14.

Calvano, E., G. Calzolari, V. Denicolo, and S. Pastorello (2020): "Artificial intelligence, algorithmic pricing, and collusion," *American Economic Review*, 110, 3267–97.

Chen, Y. (2002): "A family of supermodular Nash mechanisms implementing Lindahl allocations," *Economic Theory*, 19, 773–790.

Competition Bureau (2018): "Big Data and Innovation: Implications for Competition Policy in Canada," Discussion paper.

Dasgupta, P., P. Hammond, and E. Maskin (1979): "The Implementation of Social Choice Rules: Some General Results on Incentive Compatibility," *The Review of Economic Studies*, 46, 185–216.

di Bernardo, M., C. Budd, A. R. Champneys, and P. Kowalczyk (2008): *Piecewise-smooth dynamical systems: theory and applications*, vol. 163, Springer Science & Business Media.

Erev, I., Y. Bereby-Meyer, and A. E. Roth (1999): "The effect of adding a constant to all payoffs: experimental investigation, and implications for reinforcement learning models," *Journal of Economic Behavior & Organization*, 39, 111–128.

Erev, I. and A. E. Roth (1998): "Predicting How People Play Games: Reinforcement Learning in Experimental Games with Unique, Mixed Strategy Equilibria," *The American Economic Review*, 88, 848–881.

Filippov, A. F. (1988): *Differential Equations with Discontinuous Right-Hand Sides*, Springer Science & Business Media.

Friedman, D. and R. Oprea (2012): "A Continuous Dilemma," *American Economic Review*, 102, 337–63.

Gomes, E. R. and R. Kowalczyk (2009): "Dynamic Analysis of Multiagent Q-Learning with ϵ-Greedy Exploration," in *Proceedings of the 26th Annual International Conference on Machine Learning*, 369–376.

Halfin, S. and W. Whitt (1981): "Heavy-traffic limits for queues with many exponential servers," *Operations research*, 29, 567–588.

Hansen, K., K. Misra, and M. Pai (2021): "Algorithmic Collusion: Supra-Competitive Prices via Independent Algorithms," *Marketing Science*, 40, 1–12.

Harrison, J. M. and M. I. Reiman (1981): "Reflected Brownian motion on an orthant," *The Annals of Probability*, 9, 302–308.

Hopkins, E. and M. Posch (2005): "Attainability of boundary points under reinforcement learning," *Games and Economic Behavior*, 53, 110–125.

Iglehart, D. L. (1965): "Limiting diffusion approximations for the many server queue and the repairman problem," *Journal of Applied Probability*, 2, 429–441.

Klein, T. (2021): "Autonomous algorithmic collusion: Q-learning under sequential pricing," *The RAND Journal of Economics*, 52, 538–558.

Kühn, K.-U. and S. Tadelis (2018): "The Economics of Algorithmic Pricing: Is collusion really inevitable?" Working paper.

Kurtz, T. G. (1970): "Solutions of ordinary differential equations as limits of pure jump Markov processes," *Journal of Applied Probability*, 7, 49–58.

Lamba, R. and S. Zhuk (2022): "Pricing with Algorithms," working paper.

Leisten, M. (2022): "Algorithmic Competition, with Humans," Working paper.

Leonardos, S. and G. Piliouras (2022): "Exploration-exploitation in multi-agent learning: Catastrophe theory meets game theory," *Artificial Intelligence*, 304.

Lerer, A. and A. Peysakhovich (2017): "Maintaining cooperation in complex social dilemmas using deep reinforcement learning," *arXiv preprint arXiv:1707.01068*.

Mathevet, L. (2010): "Supermodular mechanism design," *Theoretical Economics*, 5, 403–443.

Mertikopoulos, P. and W. H. Sandholm (2016): "Learning in games via reinforcement and regularization," *Mathematics of Operations Research*, 41, 1297–1324.

Mitzenmacher, M. (2001): "The power of two choices in randomized load balancing," *IEEE Transactions on Parallel and Distributed Systems*, 12, 1094–1104.

Musolff, L. A. (2021): "Algorithmic Pricing Facilitates Tacit Collusion: Evidence from E-Commerce," Working paper.

OECD (2017): "Algorithms and Collusion: Competition Policy in the Digital Age," Technical report.

Parkes, D. C. (2004): "On learnable mechanism design," in *Collectives and the Design of Complex Systems*, Springer, 107–131.

Sandholm, W. H. (2005): "Negative externalities and evolutionary implementation," *The Review of Economic Studies*, 72, 885–915.

Tumer, K. and N. Khani (2009): "Learning from actions not taken in multiagent systems," *Advances in Complex Systems*, 12, 455–473.

Tuyls, K., P. J. Hoen, and B. Vanschoenwinkel (2005): "An Evolutionary Dynamical Analysis of Multi-Agent Learning in Iterated Games," *Autonomous Agents and Multi-Agent Systems*, 12, 115–153.

Tuyls, K. and G. Weiss (2012): "Multiagent learning: Basics, challenges, and prospects," *Ai Magazine*, 33, 41–41.

Wager, S. and K. Xu (2021): "Diffusion asymptotics for sequential experiments," *arXiv preprint arXiv:2101.09855*.

Wein, L. M. (1992): "Dynamic scheduling of a multiclass make-to-stock queue," *Operations Research*, 40, 724–735.

Wunder, M., M. L. Littman, and M. Babes (2010): "Classes of Multiagent Q-learning Dynamics with epsilon-greedy Exploration," in *Proceedings of the 27th Annual International Conference on Machine Learning*, 1167–1174.

Appendix A

We restate Theorem 1 in its more formal version.

Theorem (1). *Let (θ, π) be a collection of adaptive agents that satisfy Assumption A1 individually, and let the domain $K \subset \mathbb{R}^{\times_i d_i}$ of θ be a compact set. Let $(H_j)_{j \in J}$ be the collection of θ's maximal Lipschitz-continuity domains, that is, let H_j be the largest open set such that θ is Lipschitz over H_j and there is a discontinuity on $\overline{H}_j$. For all $j \in J$ the collection of Cauchy problems*

$$\begin{cases} \frac{d\Theta^i(t)}{dt} = \alpha \mathbb{E}_{\pi^i, \pi^{-i}} \left[T^i(\pi^i, r(\pi^i, \pi^{-i}), \Theta^i(t)) \right] \\ \Theta^i(0) = y_0^i \end{cases}$$

has a solution Θ^i for all i over H_j for all $y_0 \in H_j$. There exists a sequence of processes $\{\theta_n\}_{n \in \mathbb{N}}$ such that:

- $\mathbb{E}[\theta_1(\tau(k))] = \mathbb{E}[\theta(k)]$ *for all k, $\tau(k) = \inf\{t \mid \theta_1(t)$ jumped k times$\}$,*
- *the infinitesimal generators $\mathcal{A}T_n(\theta)$ are all identical to $\mathcal{A}T_1(\theta)$ for all $\theta \in H_j$ and n,*
- $\lim_{n \to \infty} P\left\{ \sup_{t \leq T} \left\| \theta_n(t) - \Theta(t) \right\| > \eta \right\} = 0$ *for all $T \geq 0$ and $\eta > 0$ such that $\{\Theta(t)\}_{t \leq T} \subset H_j$.*

Proof of Theorem 1. The existence of a solution for the Cauchy problem is guaranteed by Assumption A1 and the restriction to the maximal continuity domains H_j. In particular, notice that one can write $T^i(\pi^i(\theta), r(\pi^i(\theta^i), \pi^{-i}(\theta^{-i}), \theta^i)$ as a map $\hat{T}(\theta, Y)$ where Y is a random variable representing the uncertainty introduced by the policies π.

We can divide the proof of Theorem 1 in two main steps:

1. Finding the correct continuous-time embedding of the adaptive algorithm θ;
2. Identifying a scaling that guarantees limits are well-defined.

First, let us fix a compact ball of radius r in $\mathbb{R}^{\times_i d_i}$. We will consider the set $E = H \cap B(r)$ with the Borel intersection sigma algebra. Since we can choose r to be as large as we want, the approximation will hold for any finite values of θ. Let us add one component to the vector θ, in position $\times_i d_i + 1$, which will keep track of the iteration k.

As far as the first step is concerned, let us define a Poisson process N_1 of rate $\lambda_1 = 1$. Consider the sequence of (stochastic) arrival times $0 < \tau_1 < \tau_2 < \tau_3 < \ldots$. We define the process $\theta_1(t)$ as

$$\theta_1(t) = \theta(k) \qquad \text{if } \tau_{k+1} > t \geq \tau_k$$

for all times $t \geq 0$. The process $\theta_1(t)$ is a compound Poisson process, cadlag and Markov. Naturally, its $\times_i d_i + 1$ component always coincides with the iteration k. At arrival times the adaptive algorithm is equal to its continuous time equivalent θ_1, which proves item 1 of the Theorem.

We now want to increase the pace of the updates while retaining the same uncertainty in expectation. Intuitively, we can "speed up" the Poisson arrivals, but we also need to "dampen" the jumps accordingly, otherwise the process will diverge to infinity. Formally, we consider a sequence of Continuous-Time Markov Chains indexed by $n \in \mathbb{N}$ as follows:

- The jump rate λ_n is defined as $\lambda_n = n$.
- At each jump, the update in the first $\times_i d_i$ components is[10]

$$\theta_n(t) - \theta_n(t^-) = \frac{1}{n}\hat{T}(\theta_n(t^-), Y)$$

- At each jump, the update in the coordinate $\times_i d_i + 1$ is

$$\theta_n(t) - \theta_n(t^-) = \frac{1}{n}$$

Intuitively, the updates of the original process θ are scaled down by a factor n and the last coordinate keeps track of how many updates have occurred scaled by n.

Consider then the measure $\mu^n(x, dz)$ of updates at x, with

$$\mu_n(x, dz) = \mathbb{P}\Big\{\theta_n(\tau_n) \in dz | \theta_n(0) = x\Big\}$$

where τ_n is the first exit time of θ_n from x. We define the component-wise function

$$F_n(x)^m = \lambda_n \int (z^m - x^m)\mu_n(x, dz), \tag{5}$$

which intuitively describes the expected jump of θ_n from x along the m-th component over one unit of time. In fact, F_n can be rewritten as

$$F_n(x)^m = n \int \frac{\alpha}{n}\hat{T}^m(x, Y)\mu = \int \alpha \hat{T}^m(x, Y)\mu.$$

We chose the scaling in such a way that the function F_n is independent of n. The function F_n is exactly the infinitesimal generator of the compound Poisson process $\theta_n(t)$, therefore

[10]Note that we omit the dependence on the iteration since iterations are now part of the process θ^n.

item (2) of the Theorem is proved.

Let $F(x) := \lim_{n\to\infty} F_n(x)$. It is clear that $F(x) = F_n(x)$ for all n. Moreover the function $F(x)$ is Lipschitz in every component. We will need a technical lemma:

Lemma 1. *Let E be a compact set in $\mathbb{R}^{|\mathcal{I}|\times|\mathcal{S}|\times|\mathcal{A}|}$. There exists a sequence $\{\varepsilon_n\}_n > 0$ with $\lim_{n\to\infty} \varepsilon_n = 0$ such that*

$$\lim_{n\to\infty} \sup_{x\in E} \lambda_n \int_{|z-x|>\varepsilon_n} |z-x|\mu_n(x,dz) = 0$$

Moreover,

$$\sup_n \sup_{x\in E} \lambda_n \int_E |z-x|\mu_n(x,dz) < \infty$$

Proof. Since E is compact $\hat{T}(\theta, Y)$ must be bounded. Let $M = \sup_{\theta\in E} T(\theta, Y)$ across dimension, and note that $M < +\infty$. Let then $\{\frac{M}{n}\}_n$ be a sequence satisfying the assumptions of the Lemma, and notice that $\int_{|z-x|>\varepsilon_n} |z-x|\mu_n(x,dz) = 0$ for all x and n. We thus proved the first claim. The second claim follows a simple observation: $|z-x|\mu_n(x,dz) \leq \frac{M}{n}$ for all x. Since $\lambda_n = n$, we obtain that

$$\sup_n \sup_{x\in E} \lambda_n \int_E |z-x|\mu_n(x,dz) = M < \infty$$

which concludes the proof. □

This lemma verifies one of the conditions of the following Theorem by Kurtz (1970):

Theorem 2.11. *Suppose there exists $E \subset \mathbb{R}^k$, a function $F\colon E \to \mathbb{R}^k$ and a constant M such that $|F(x) - F(y)| \leq M|x-y|$ for all $x, y \in E$ and*

$$\lim_{n\to\infty} \sup_{x\in E_n\cup E} |F_n(x) - F(x)| = 0$$

Let $X(t,x_0), 0 \leq t \leq T, x_0 \in E$ satisfy

$$X(0,x_0) = x_0, \qquad \dot{X}(t,x_0) = F(X(t,x_0))$$

Suppose additionally that the sequence F_n satisfies the conditions of Lemma 1, then for every $\eta > 0$

$$\lim_{n\to\infty} P\Big\{\sup_{t\leq T} |X_n(t) - X(t,x_0)| \geq \eta\Big\} = 0$$

If $X(t,x_0) = \Theta$, we can verify that the assumptions of the Theorem hold:

- since $\hat{T}$ is Lipschitz, and $F_n = F$ are integrals of Lipschitz functions, it is clear that $|F(x) - F(y)| \leq M|x - y|$ holds,
- $\lim_n \sup_{x \in H} |F_n(x,t) - F(x,t)| = 0$ is satisfied by definition of $F_n = F$,
- the conditions of *Lemma* 1 are verified.

Then, Theorem 2.11 implies that for every $\eta > 0$

$$\lim_{n \to \infty} P\Big\{ \sup_{t \leq T} |\theta_n(t) - \Theta(t)| \geq \eta \Big\} = 0$$

which proves item 3 of the Theorem and concludes the proof.

As advanced at the beginning, the process Θ is a deterministic process with all uncertainty collapsed into the drift component. □

Proof of Proposition 1 The existence of the equilibrium q_D^{eq} follows directly from setting the field over $\omega_{D,D}$ to zero.

We prove existence of q_C^{eq} and its related property for one agent; by symmetry, the other agent's Q-values enjoy the same properties. The boundary is defined as $\Sigma = \{q \in \mathbb{R}^2 \colon c \cdot q = 0\}$ where $c = (1, -1)$ and $\cdot$ denotes the usual dot product. Using the Filippov convention, we can further divide Σ in three regions:

- a *crossing region*, $\Sigma^c = \{q \colon (c \cdot (A_C q + b_C))(c \cdot (A_D q + b_D)) > 0\}$
- a *repulsive region*, $\Sigma^r = \{q \colon c \cdot (A_C q + b_C) > 0,\ c \cdot (A_D q + b_D) < 0\}$
- a *sliding region*, $\Sigma^s = \{q \colon c \cdot (A_C q + b_C) < 0,\ c \cdot (A_D q + b_D) > 0\}$

where we have

$$A_C = \begin{bmatrix} \alpha\left(1 - \frac{\varepsilon}{2}\right)(\gamma - 1) & 0 \\ \alpha\gamma\frac{\varepsilon}{2} & -\alpha\frac{\varepsilon}{2} \end{bmatrix} \qquad A_D = \begin{bmatrix} -\alpha\frac{\varepsilon}{2} & \alpha\gamma\frac{\varepsilon}{2} \\ 0 & \alpha\left(1 - \frac{\varepsilon}{2}\right)(\gamma - 1) \end{bmatrix},$$

and

$$b_C = \begin{bmatrix} \alpha\left(1 - \frac{\varepsilon}{2}\right)\left(2 - \frac{\varepsilon}{2}\right)g \\ \alpha\frac{\varepsilon}{2}\left(2 + g - g\frac{\varepsilon}{2}\right) \end{bmatrix} \qquad b_D = \begin{bmatrix} \alpha\left(1 + \frac{\varepsilon}{2}\right)\frac{\varepsilon}{2}g \\ \alpha\left(1 - \frac{\varepsilon}{2}\right)\left(2 + \frac{\varepsilon}{2}g\right) \end{bmatrix}.$$

We can define the sliding solution as the field $\frac{d\mathbf{Q}}{dt} = F^s(\mathbf{Q})$ over the sliding region where

$$F^s(\mathbf{Q}) = \frac{c\cdot(A_D\mathbf{Q}+b_D)(A_C\mathbf{Q}+b_C) - c\cdot(A_C\mathbf{Q}+b_C)(A_D\mathbf{Q}+b_D)}{c\cdot(A_D\mathbf{Q}+b_D) - c\cdot(A_C\mathbf{Q}+b_C)}$$

The relative time spent on $\omega_{C,C}$ at point $\mathbf{Q}$ is defined as

$$\tau_C = \frac{c\cdot(A_D\mathbf{Q}+b_D)}{c\cdot(A_D\mathbf{Q}+b_D) - c\cdot(A_C\mathbf{Q}+b_C)}$$

The sliding vector field becomes

$$\frac{d\mathbf{Q}_j}{dt} = \frac{\alpha\left(\frac{1}{2}\varepsilon g(2-\varepsilon)(g-1) + (2g+(\gamma-1)\mathbf{Q}_j)(2+(\gamma-1)\mathbf{Q}_j)\right)}{2(1+g+(\gamma-1)\mathbf{Q}_j)}$$

for every direction j. By setting the field equal to zero and solving for $\mathbf{Q}_j$, we find that there is an equilibrium at

$$q_{C,j}^{eq} = \frac{1+g-\sqrt{(g-1)(g-1-\varepsilon g+\frac{\varepsilon^2 g}{2})}}{(\gamma-1)}$$

for all j. This equation has a feasible solution for all $\varepsilon < 1-\sqrt{\frac{2-g}{g}}$. □

Proof of Corollary 1. The result follows immediately from the proof of Proposition 1. In particular, it is sufficient to compute

$$\tau_C = \frac{c\cdot(A_D\mathbf{Q}+b_D)}{c\cdot(A_D\mathbf{Q}+b_D) - c\cdot(A_C\mathbf{Q}+b_C)}$$

at $\mathbf{Q} = q_C^{eq}$. □

Proof of Theorem 2. First off, note that there is a given ordering of rewards in a Prisoner's Dilemma:

$$r(D,C) > r(C,C) > r(D,D) > r(C,D)$$

We will prove existence of an equilibrium of the following system:

$$\begin{cases} \dot{\theta}^C = \alpha\left[U(\theta^C, r(C,C)) + V(\theta)\right] \\ \dot{\theta}^D = (1-\alpha)\left[U(\theta^D, r(D,C)) + V(\theta)\right] \end{cases}$$

in the half-plane where C is the preferred action, and

$$\begin{cases} \dot{\theta}^C = (1-\alpha)\left[U(\theta^C, r(C,D)) + V(\theta)\right] \\ \dot{\theta}^D = \alpha\left[U(\theta^D, r(D,D)) + V(\theta)\right] \end{cases}$$

in the half-plane where D is the preferred action. Note that we are assuming WLOG that the learning speeds sum to 1, since all it matters is the relative speed of learning. To start, let us assume α is identical across the half planes.

We want to show that there exist an α and a θ^* such that:

$$\begin{cases} \alpha U(\theta^*, r(C,C)) + (1-\alpha)U(\theta^*, r(C,D)) + V(\theta^*) = 0 \\ (1-\alpha)U(\theta^*, r(D,C)) + \alpha U(\theta^*, r(D,D)) + V(\theta^*) = 0 \end{cases} \tag{6}$$

Because we used the same α on both sides, we are simply looking for a translation of Equation (6), therefore we can develop the argument disregarding the $V(\theta^*)$ component. For a given θ, we can write this problem as a convex combination of two vectors:

$$\alpha\vec{x} + (1-\alpha)\vec{y} = \vec{0}$$

where

$$\vec{x}(\theta) = \begin{bmatrix} U(\theta, r(C,C)) \\ U(\theta, r(D,D)) \end{bmatrix} \qquad \vec{y}(\theta) = \begin{bmatrix} U(\theta, r(C,D)) \\ U(\theta, r(D,C)) \end{bmatrix}$$

Let θ^1 be the value of θ such that $U(\theta^1, r(C,C)) = 0$. Then, using the monotonicity of U in rewards, the two vectors $\vec{x}, \vec{y}$ computed in θ^1 will be positioned as in Figure 10. Let θ^2 instead be the value of θ such that $U(\theta^2, r(C,D)) = 0$. Again, the two vectors $\vec{x}, \vec{y}$ are positioned as in Figure 10. Notice that by monotonicity of U in its first component, $\theta^1 > \theta^2$. The same assumption guarantees that the lines $\vec{y}(\theta_1 + (\theta_2 - \theta_1)t)$ and $\vec{x}(\theta_1 + (\theta_2 - \theta_1)t)$ lie on the left and right of the vertical axis, respectively.

Define $f : [0,1] \to \mathbb{R}^2$ as

$$f(t) = \begin{cases} (1-4t)\vec{x}(\theta^1) + 4t\vec{y}(\theta^1) & t \in \left[0, \frac{1}{4}\right] \\ \vec{y}\Big(\theta^1 + (\theta^2 - \theta^1)(4t-1)\Big) & t \in \left[\frac{1}{4}, \frac{1}{2}\right] \\ (3-4t)\vec{y}(\theta^2) + (4t-2)\vec{x}(\theta^2) & t \in \left[\frac{1}{2}, \frac{3}{4}\right] \\ \vec{x}\Big(\theta^1 + 4(\theta^2 - \theta^1)(1-t)\Big) & t \in \left[\frac{3}{4}, 1\right] \end{cases}$$

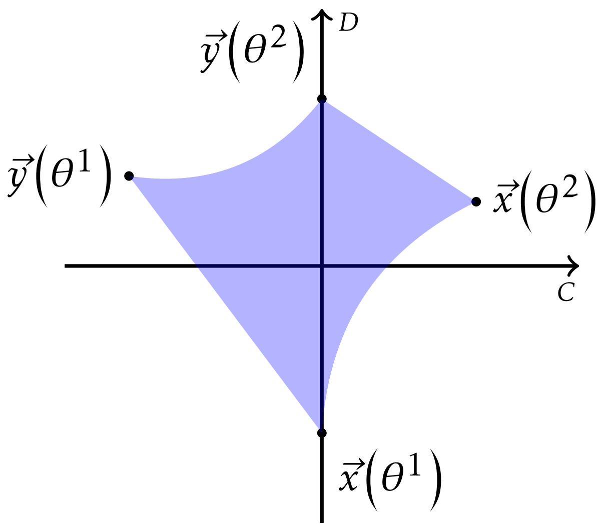

$\vec{y}\left(\theta^2\right)$
D
$\vec{y}\left(\theta^1\right)$
$\vec{x}\left(\theta^2\right)$
C
$\vec{x}\left(\theta^1\right)$

Figure 10: Homotopy

Note that, by continuity of U, $f(t)$ is a loop based in $x(\theta^1)$. We can show that f is null-homotopic by providing the following simple homotopy $H\colon [0,1]\times[0,1]\to\mathbb{R}^2$.

$$H(t,s)=\begin{cases}(1-4ts)\vec{x}(\theta^1)+4ts\vec{y}(\theta^1) & t\in\left[0,\frac{1}{4}\right]\\ (1-s)\vec{x}\left(\theta^1+s(4t-1)(\theta^2-\theta^1)\right)+s\vec{y}\left(\theta^1+s(4t-1)(\theta^2-\theta^1)\right) & t\in\left[\frac{1}{4},\frac{1}{2}\right]\\ (1-s(3-4t))\vec{x}\left((1-s)\theta^1+s\theta^2\right)+s(3-4t)\vec{y}\left((1-s)\theta^1+s\theta^2\right) & t\in\left[\frac{1}{2},\frac{3}{4}\right]\\ \vec{x}\left(\theta^1+4s(\theta^2-\theta^1)(1-t)\right) & t\in\left[\frac{3}{4},1\right]\end{cases}$$

We verify that H is a homotopy between $f(t)$ and the constant path at $\vec{x}(\theta^1)$.

- $H(0,s)=H(1,s)=\vec{x}(\theta^1)$
- $H(t,0)=\vec{x}(\theta^1)$
- $H(t,1)=f(t)$

Suppose now that there is no pair t,s such that $H(t,s)=(0,0)$. Then, by continuity it must be the case that there is an open neighborhood $V\ni(0,0)$ such that for all points $z\in V$, $z\notin Im(H)$. Note that we can restrict the loop f to a the domain $\mathbb{R}^2\setminus V$, and because $V\notin Im(H)$ we can restrict the homotopy to a homotopy $H\colon[0,1]^2\to\mathbb{R}^2\setminus V$. Thus we proved that a loop around the open set V is null-homotopic, which is equivalent to proving that $\mathbb{R}^2\setminus V$ is simply connected, a contradiction.

Therefore, there exists a pair $\bar{t},\bar{s}$ such that $H(\bar{t},\bar{s}) = (0,0)$. There is a bijective transformation between t,s and θ,α over their respective domains, which guarantees that the system of Equation (6) is satisfied.

Notice that we allowed for $\alpha \in (0,1)$ so far. However, it makes little sense to allow for $\alpha < \frac{1}{2}$: the algorithm would learn about actions it considers suboptimal faster than those he considers best. Fortunately, we observe the following:

$$\frac{1}{2}U(\theta,r(C,C)) + \frac{1}{2}U(\theta,r(C,D) < \frac{1}{2}U(\theta,r(D,C)) + \frac{1}{2}U(\theta,r(D,D).$$

This inequality follows from the ordering of rewards in a Prisoner's Dilemma game. This in particular implies that the line $\frac{1}{2}\vec{x}(\theta_1 + (\theta_2 - \theta_1)t) + \frac{1}{2}\vec{y}(\theta_1 + (\theta_2 - \theta_1)t)$ lies above the 45 degree line. Thus, we can restrict the homotopy to the parameter space $\alpha \in [\frac{1}{2}, 1]$ without affecting the result. This guarantees the existence of a parameter $\alpha > \frac{1}{2}$ which sets the sliding vector field to zero.

Now, notice that in the previous construction in Equation (6) we solved for α and θ^* such that the local time was equal on both sides of the switching boundary. We can relax this assumption so that Equation (6) becomes

$$\begin{cases} \alpha\tau U(\theta^*,r(C,C)) + (1-\alpha)(1-\tau)U(\theta^*,r(C,D)) = 0 \\ (1-\alpha)\tau U(\theta^*,r(D,C)) + \alpha(1-\tau)U(\theta^*,r(D,D)) = 0. \end{cases} \tag{7}$$

Following the previous construction, we get

$$\vec{x}(\theta) = \begin{bmatrix} \tau U(\theta,r(C,C)) \\ (1-\tau)U(\theta,r(D,D)) \end{bmatrix} \qquad \vec{y}(\theta) = \begin{bmatrix} (1-\tau)U(\theta,r(C,D)) \\ \tau U(\theta,r(D,C)) \end{bmatrix}$$

The points $\vec{x}(\theta_i),\vec{y}(\theta_i)$ for $i = 1,2$ each remain on their respective quadrants, enabling us to construct the same, rescaled, homotopy for this case. Therefore, for each τ we can identify a pair $\alpha^\tau,\theta^*(\tau)$ such that Equation (7) is satisfied.

Not all solutions to Equation (7) are steady-states however. Recall from our construction in Section 3 that we need to verify a sliding condition: the normal components of the two vector fields to the switching surface must have opposite sign and must be attractive. In equations, this translates to the following system which needs to be satisfied:

$$\begin{cases} (1-\alpha^\tau)\tau U(\theta^*(\tau),r(D,C)) - \alpha\tau U(\theta^*(\tau),r(C,C)) \geq 0 \\ \alpha^\tau(1-\tau)U(\theta^*(\tau),r(D,D)) - (1-\alpha^\tau)(1-\tau)U(\theta^*(\tau),r(C,D)) \leq 0. \end{cases} \tag{8}$$

We need a preparatory lemma:

Lemma 2. *The only region of θ where Equation (7) can be verified is such that*

$$U(\theta, r(D,C)) > U(\theta, r(C,C)) \geq 0 > U(\theta, r(D,D)) > U(\theta, r(C,D))$$

Proof. The statement follows immediately from inspection of Figure 10. Since the path $\vec{y}(\theta_1 + (\theta_2 - \theta_1)t)$ for all t falls within the second quadrant, any $\vec{x}(\theta^*)$ which satisfies Equation (7) must fall within the fourth quadrant, which directly implies the result. □

Now, rearranging Equation (7) we derive the following equalities:

$$\begin{cases} -(1-\alpha^\tau)(1-\tau)U(\theta^*(\tau), r(C,D)) = \alpha^\tau \tau U(\theta^*(\tau), r(C,C)) \\ -(1-\alpha^\tau)\tau U(\theta^*(\tau), r(D,C)) = \alpha^\tau (1-\tau) U(\theta^*(\tau), r(D,D)) \end{cases}$$

Substituting these in Equation (8) and rearranging, we obtain

$$\begin{cases} \alpha^\tau \tau U(\theta^*(\tau), r(C,C)) + \alpha^\tau (1-\tau) U(\theta^*(\tau), r(D,D)) \leq 0 \\ \alpha^\tau (1-\tau) U(\theta^*(\tau), r(D,D)) + \alpha^\tau \tau U(\theta^*(\tau), r(C,C)) \leq 0 \end{cases}$$

Thus, only one condition needs to be satisfied to guarantee sliding:

$$\tau U(\theta^*(\tau), r(C,C)) + (1-\tau) U(\theta^*(\tau), r(D,D)) \leq 0$$

Lemma 2 guarantee that a solution to this inequality exists for τ sufficiently close to 0. In particular, there exists a $\overline{\tau}$ such that for all $\tau \leq \overline{\tau}$ we obtain sliding. Therefore there exists an open set of parameters $\{\alpha^\tau \mid \tau \leq \overline{\tau}\}$ such that a sliding steady-state exists. Now, we can perturb the value of α on either side of the sliding boundary. The region we derived depends continuously from α, in particular from α^C and α^D. Therefore, the same result holds for small perturbations of α into different α^C and α^D, concluding the proof of the Theorem.

□

Proof of Theorem 3. We set to prove that, in the limit, the statistic θ^n of the dominant action dominates the statistic θ^i of any other non-dominant action. First of all, since α^{a_i} is identical across actions, the evolution in time of θ is shifted by $V(\theta)$, but V won't affect the relative rankings of the actions' estimates. Therefore, we drop V in the rest of the proof, and we focus on U.

Regardless of the opponent's policy, the reinforcer in every step observes a return in hindsight for every action. We denote by $r_n(t)$ the return from playing action n in period t, whatever the opponents' actions are. We consider the evolution of the weights pairwise: θ^n and θ^i for all i. By assumption, for any sequence of actions taken by the opponent(s), $r_n(t) \geq r_i(t)$. In particular, Assumption A3 guarantees that there exists a $T > 0$ such that $r_n(t) > r_i(t)$ for any $t > T$. Thus, in the limit the derivative $\dot{\theta}^n$ strictly dominates $\dot{\theta}^i$ in each point (x,t): $U(x, r_n(t)) > U(x,, r_i(t))$. In particular, there exists a ε such that $U(x, r_n(t)) > U(x,, r_i(t)) + \varepsilon$.

Suppose now that for some $t \geq 0$, $\theta^n(t) \geq \theta^i(t)$. We prove that it can never be the case that $\theta^i(T) > \theta^n(T)$ for some $T > t$. $\theta^n(t)$ is a solution to the ODE given by $\dot{\theta}^n(t) = U(\theta^n(t), r_n(t))$ and

$$U(\theta^n(t), r_n(t)) \geq U(\theta^n(t), r_i(t)) = U(\theta^i(t), r_i(t))$$

Thus, $\dot{\theta}^i(t) \leq U(\theta^i(t), r_n(t))$. The fundamental theorem of differential inequalities guarantees that the solution $\theta^i(T)$ is bounded above by $\theta^n(T)$ for all $T > t$ on its maximal domain.

Consider instead the case where $\theta^i(T) > \theta^n(T)$. From the definition of Reinforcer, we have that

$$U(\theta^i(T), r_i(T)) \leq U(\theta^i(T), r_n(T)) < U(\theta^n(T), r_n(T))$$

We want to show that there exists a $t > T$ such that $\theta^n(t) = \theta^i(t)$. To this end, suppose by contradiction that $\forall t > T$, $\theta^i(t) > \theta^n(t)$. Observe that the previous inequalities imply that

$$\left.\frac{d}{ds}\right|_{s=t} (\theta^i(s) - \theta^n(s)) < 0 \qquad \forall t > T. \tag{9}$$

Then, $(\theta^i(t) - \theta^n(t))$ is a monotone decreasing function of time. Because the algorithm is bounded, it must be the case that

$$\lim_{t \to +\infty} (\theta^i(t) - \theta^n(t)) = b \geq 0. \tag{10}$$

From the definition of limit and the monotonicity of the derivative, for any ϵ there exists a $t' > T$ such that, for all $t > t'$,

$$\theta^n(t) + b \leq \theta^i(t) < \theta^n(t) + b + \epsilon.$$

Thus, strict monotonicity of the reinforcer's update implies that there exists a $\delta > 0$ such that

$$U(\theta^i(t), r_i(t)) \leq U(\theta^n(t), r_i(t)) < U(\theta^n(t), r_n(t)) + \delta. \tag{11}$$

Note that, by Equation (10) and the monotonicity given by Equation (9), the limit of the derivative of the difference $\theta - \theta^n$ must converge to 0:

$$\lim_{t\to+\infty} (\theta^i(t) - \theta^n(t))' = \lim_{t\to+\infty} (U(\theta^i(t), r_i(t)) - U(\theta^n(t), r_n(t)))' = 0$$

This is a contradiction of Equation (11). Then, there must exist a T such that $\theta^i(T) = \theta^n(T)$. From the first part of the proof, this implies that $\forall t > T$ we have $\theta^i(T) \leq \theta^n(T)$, and this completes the proof, □

Proof of Theorem 4. The proof is largely based upon Theorem 3. We will show that there is always a $\mathcal{T}$ such that the actions taken after $\mathcal{T}$ survive an IESDS procedure.

Let a_i be a strategy for player i which is dominated by b_i in the game G. With the same argument of the proof of Theorem 3 we can show that it must be the case that, in the limit, $\theta^{b_i} > \theta^{a_i}$. Equivalently, there exists a $\mathcal{T}_1$ such that for all $t \geq \mathcal{T}_1$ we have $\theta^{b_i}(t) > \theta^{a_i}(t)$. Therefore, after time $\mathcal{T}_1$ it is as if the agents were playing in a reduced game $G^1 = (N, (A_i^1)_i, (u_i)_i)$, where $A_i^1 = A_i \setminus \{a_i\}$ and $A_j^1 = A_j$ for all $j \neq i$.[11] We can now apply the same idea to this new reduced game G^1 and eliminate a strictly dominated strategy in this reduced game. While IESDS eliminates strategies "in place", the algorithms abandon dominated strategies over time, reducing the effective game played. Of course, the components of θ that correspond to dominated actions keep getting updated, but note that if an action is dominated given a larger subset of opponent's strategies, it is also (weakly) dominated given a smaller subset. Therefore, following the usual differential inequality argument, the θ corresponding to a dominated action will always remain below that of actions surviving IESDS. We then define $\mathcal{T}$ as the largest among the $\mathcal{T}_k$ that correspond to an action being eliminated, and this concludes the proof. □

Appendix B

In this Appendix we discuss the chaotic theory of the system in Section 3. Chaos theory studies non-linear systems whose trajectories appear stochastic but are the result of deterministic laws of motion. The most commonly accepted definition of chaotic behavior

[11] Of course, Assumption A3 guarantees that even action a_i will be played with some positive probability, but the statement of Theorem 4 guarantees that the probability is small enough to not affect the order of the expected rewards.

is high sensitivity to small perturbations in initial conditions. We plot a sample trajectory of the system in Figure 11. The system behaves erratically and unpredictably along its deterministic trajectory, and it is highly sensitive to its initial condition. The "butterfly" traced by the trajectory appears hard to characterize. However, the heatmap shows that most of the time is spent in a region where the estimates of cooperation and defection coincide.

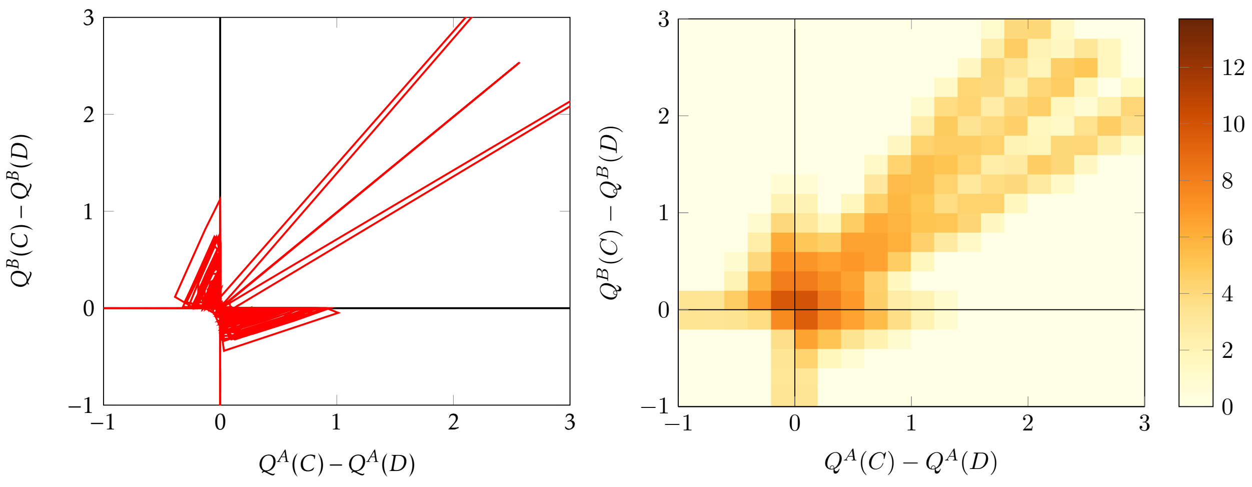

Figure 11: A chaotic trajectory of the system of Equation (4) in a 2-D representation. On the left, we depict the motion in the difference space. Agents appear chaotically attracted to a butterfly-like motion around the origin. The figure on the right represents the logarithmic density of time spent in a given square cell of side 0.2. Effectively, over 90% of time is spent in the square centered on the origin.

Figure 12 shows the effect of a small initial perturbation on two trajectories of the 4-D system along its first component.

The deterministic chaos we observe makes anly stability analysis impossible. However, as shown in Figure 11, the system spends most of its time in a region near the double sliding boundary. That is, most of the time the system will show equal values for cooperation and defection for both Alice and Bob. The sliding analysis we carried out in the symmetric case is not too far off the mark in the 4-D case as well, as one can see in Figure 6b: the gap between the predicted local time and the realized local time is due to the asymmetry that always arises in the discrete algorithmic system.

Moreover, the double sliding plane is locally attractive. When both agents cooperate, both are drawn towards defection, and thus towards sliding. Suppose Alice is the first to hit the switching surface, and thus to slide. Bob's vector fields adapt to Alice's new, sliding behavior, but the switching surface retains its attractivity. Bob will join Alice in

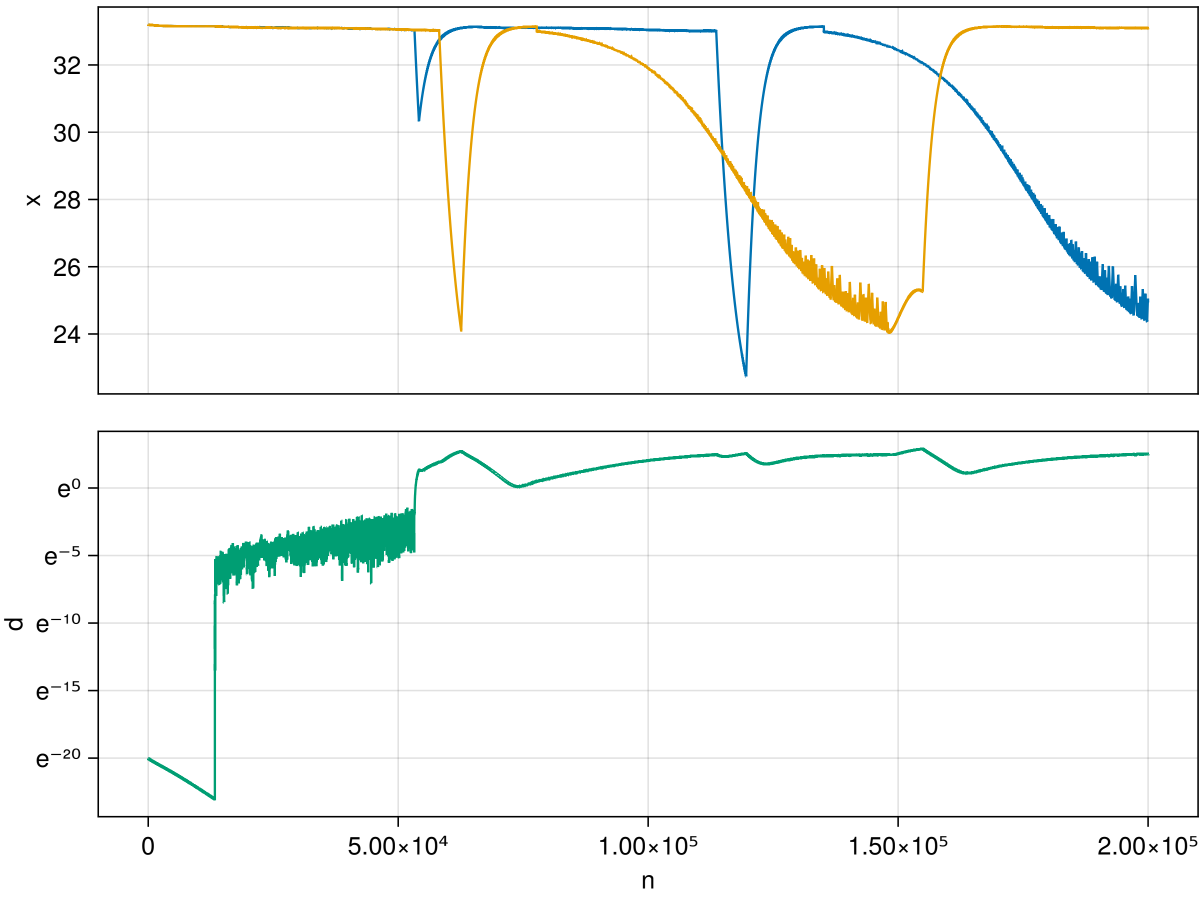

Figure 12: The top figure depicts the evolution of (the first component of) two trajectories with minimal perturbations of their initial conditions. The bottom figure represents the absolute distance between these two trajectories, in logarithmic scale. After an initial convergence, hitting the boundary leads to exponential divergence (the green line has constant slope upwards in the logarithmic scale). Finally the trajectories saturate, i.e. the boundedness of trajectories limits their absolute divergence.

sliding, unless Alice will already have left the switching surface. Either Alice or Bob will however exit from the 2-dimensional sliding plane. The coordination bias's cycles take place in 4 dimensions — they do not collapse on a pseudo-equilibrium.